

EFFECT OF ACCELERATED CARBONATION CURING ON PROPERTIES OF PERVIOUS CONCRETE: AN EFFECTIVE WAY OF CO₂ SEQUESTRATION AND WATER CONSERVATION

A Thesis submitted in partial-fulfillment of the requirements for the award of degree of

MASTER OF ENGINEERING IN STRUCTURAL ENGINEERING

Submitted by

Gaganjot Singh Sidhu

(801724011)

Under the Guidance of

Dr. Shweta Goyal

Associate Professor

Department of Civil Engineering



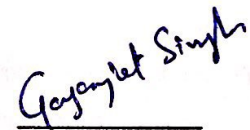
THAPAR INSTITUTE
OF ENGINEERING & TECHNOLOGY
(Deemed to be University)

**DEPARTMENT OF CIVIL ENGINEERING
THAPAR INSTITUTE OF ENGINEERING AND TECHNOLOGY
(DEEMED TO BE UNIVERSITY), PATIALA, PUNJAB
JULY, 2019**

DECLARATION

I, Gaganjot Singh Sidhu hereby declare that the work presented in this thesis entitled, “**Effect of accelerated carbonation curing on properties of pervious concrete: an effective way of CO₂ sequestration and water conservation**”, in partial fulfillment of the requirement for the award of degree of **Master of Engineering in Structural engineering** submitted at Department of Civil Engineering, Thapar Institute of Engineering and Technology (Deemed to be University), Patiala is an authentic record of my own work carried under the supervision of **Dr. Shweta Goyal, Associate Professor**, Thapar Institute of Engineering and Technology (Deemed to be University), Patiala from July, 2018 to July, 2019. The matter presented in this has not been submitted either in part or full to any other university or institute for the award of any other degree.

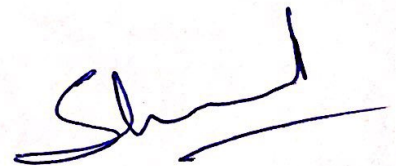
Place: PATIALA
Date: 23/8/2019



Gaganjot Singh Sidhu
Roll No: 801724011

CERTIFICATE

It is certified that the above statement made by student is correct to the best of my knowledge and belief.



Dr. Shweta Goyal
(Associate Professor)

Department of Civil Engineering
TIET (Deemed to Be University)
Patiala, Punjab

ACKNOWLEDGEMENT

It is a great pleasure for me to take this opportunity to express my profound sense of gratitude to all those who assisted me in the completion of this dissertation work. I gratefully acknowledge my supervisors **Dr. Shweta Goyal** for her understanding, encouragement and personal attention which have provided good and smooth basis for my dissertation tenure. This work would not have been possible without her guidance, support and encouragement. Under her guidance, I successfully overcame many difficulties and learned a lot. I am also thankful to **Dr. Prem Pal Bansal**, HCED and **Dr. Prakash Gopalan**, Director, TIET, Patiala for providing the facilities for the completion of my coursework.

I am thankful to lecturer **Mr. Davinder Sharma** who devoted their valuable time for the successful completion of my dissertation. I am also thankful to my friends, **Vijay hans, Rohit kumar and Virender Solanki** for their support during my dissertation. I extend my gratitude to the researchers and scholars whose hours of toil have produced the papers that I have used for my dissertation.

I would like to express my deepest gratitude to my parents and family, without whom I am nothing. To provide me with a great opportunity, everlasting support, big encouragement and lots of love.

Gaganjot Singh

Gaganjot Singh Sidhu

(801724011)

ABSTRACT

Climate change and global warming are the critical problems which today's world is facing, and carbon dioxide is a major cause of these problems. Therefore, sustainable future needs a reduction in CO₂ emissions as well as capture, storage, and consumption of already existing CO₂ to reduce its adverse effects on the environment. One of the possible ways of reducing CO₂ is through sequestration by accelerated carbonation curing (ACC). Accelerated carbonation curing is a technique in which CO₂ is sequestered by cementitious compounds. This sequestered CO₂ reacts with initial hydration products and results in the formation of calcium carbonate as one of the end products. Calcium carbonate has better mechanical properties as compared conventional hydration products and hence enhances properties of pervious concrete. Cementitious compounds are known for their ability to react with atmospheric CO₂.

ACC was used as curing technique for pervious concrete in the present study. For comparison, steam curing at 60°C and water curing regimes were also adopted. Further, in order to study the effect the duration of carbonation curing, ACC was adopted at two different carbonation duration; 6 hours and 12 hours. Further, in order to investigate the effect of different curing regimes on the microstructure of pervious concrete, SEM, XRD and TGA were conducted. The developed pervious concrete was then used to create interlocking paver blocks, and these blocks were tested for compressive strength and porosity.

ACC for 12 hours has shown the highest 7 and 28-day compressive strength, and lowest permeability and porosity among all curing regimes. This was credited to the formation of calcium carbonate during ACC, and CSH on subsequent water curing of ACC specimen. Steam cured specimens showed high porosity and permeability due to the non-homogenous distribution of hydration products and introduction of micro-cracks at elevated temperatures.

Table of Content

	Page No
CERTIFICATE	ii
ACKNOWLEDGEMENT	iii
ABSTRACT	iv
TABLE OF CONTENTS	v
LIST OF FIGURES	viii
LIST OF TABLES	ix
ABBREVIATIONS	xi
Chapter 1. Introduction	
1.1. General	1
1.2. Commonly used curing techniques	2
1.2.1. Water curing	2
1.2.2. Membrane curing	4
1.2.3. Steam curing	5
1.2.4. Accelerated carbonation curing	8
1.3. Pervious concrete	12
1.3.1. General	12
1.3.2. Advantages of pervious concrete	13
1.4. Scope of the present work	14
Chapter 2. Literature Review	

2.1.	General	15
2.2.	Compressive strength	15
2.3.	Porosity	21
2.4.	Permeability	23
2.5.	XRD Analysis	26
2.6.	SEM Analysis	30

Chapter 3. Experimental Program

3.1.	Materials	33
3.1.1.	Cement	33
3.1.2.	Coarse aggregates	34
3.1.3.	Water	36
3.2.	Mix proportions	36
3.3.	Casting	37
3.3.1.	Casting	37
3.4.	Curing	39
3.4.1.	Water curing	40
3.4.2.	Steam curing	41
3.4.3.	Accelerated carbonation curing	42
3.5.	Testing	43
3.5.1	Compressive strength	43
3.5.2.	Porosity	44
3.5.3.	Permeability test	45
3.6.	Microstructure analysis	48
3.6.1.	Thermogravimetric analysis (TGA)	48
3.6.2.	Scanning electron microscope (SEM) analysis	48

3.6.3.	XRD analysis	49
Chapter 4. Results and discussion		
4.1.	General	50
4.2.	Compressive strength	50
4.2.1.	Strength development rate	53
4.3.	Porosity	54
4.3.1.	Relationship between compressive strength and porosity	56
4.4.	Permeability	57
4.5.	Effect duration of ACC on carbonation products and CO ₂ uptake	59
4.6.	XRD analysis	60
4.7.	SEM analysis	62
4.8.	Application of developed pervious concrete in paver blocks	65
4.8.1.	Compressive strength of paver blocks	65
4.8.2.	Porosity of paver blocks	66
Chapter 5. Conclusion		
5.1.	General	68
5.2.	Compressive strength	68
5.3.	Porosity	68
5.4.	Permeability	69
5.5.	Microstructure analysis	69
5.5.1.	TGA analysis	69
5.5.2.	XRD analysis	69
5.5.3.	SEM analysis	70
5.6.	Application of pervious concrete to paver blocks	70
References		71

List of Table

S.No	List of Table	Page No
2.1	Mix proportion of different mixes	17
2.2	Compressive strength of moist cured and CO ₂ cured specimens	18
2.3	Characteristics of different mixtures of pervious concrete	19
2.4	Characteristics of different mixtures of pervious concrete	23
2.5	Permeability properties of all mixes	25
2.6	Permeability of Various Mixes	25
3.1	Chemical properties of Ordinary Portland cement (OPC)	33
3.2	Physical properties of ordinary Portland cement (OPC)	34
3.3	Physical properties of coarse aggregates	34
3.4	Sieve size analysis of Coarse Aggregates (20mm)	35
3.5	Sieve size analysis of coarse aggregates (10 mm)	35
3.6	Sieve size analysis of coarse aggregate (60% of largest size 20mm and 40% of largest size 10mm)	36
3.7	Mix proportion and 7-day compressive strength of pervious concrete trail mixes	37
3.8	Geometry of specimens used for testing different properties	39
3.9	The curing schemes and their designation	39
4.1	Compressive strength test results at the ages of 3,7 and 28-days of casting	50
4.2	Porosity test results at the ages of 3, 7 and 28-days of casting	54
4.3	Permeability test results at the ages of 3, 7 and 28-days of casting	57

4.4	Percentage of compounds present in ACC cured specimens	59
4.5	Compressive strength test results at the ages of 3,7 and 28-days of casting	66
4.6	Porosity test results at the ages of 3, 7 and 28-days of casting	67

List of Figures

S.No	List of Figures	Page No
1.1	Curing of concrete	1
1.2	Water curing by sprinkling method	3
1.3	Curing of the concrete slab by ponding method	4
1.4	Membrane curing	5
1.5	Steam curing chamber	8
1.6	Laboratory process of carbonation curing	10
1.7	Pervious concrete pavement	12
1.8	Drainage of water through pervious concrete	12
2.1	Effect of RG on the compressive strength of water and CO ₂ -cured mortars at different ages	15
2.2	Compressive strength of concrete at different pressures and durations of ACC	16
2.3	Compressive strength development with curing age	20
2.4	Effect of duration of initial steam curing at 50 °C	21
2.5	Comparison of porosity for water curing and carbonation curing for different percentages of CKD	22
2.6	Permeability of different pervious concrete mixes	24
2.7	XRD results of cement mortars cured with different curing regimes	26
2.8	XRD results of moist and ACC cured concrete cured	27
2.9	XRD analysis of different curing regimes after 3 days of casting	28

2.10	XRD patterns of moist and ACC cured samples	29
2.11	SEM micrograph of samples subjected to different duration of steam	30
2.12	SEM micrograph of the specimen exposed to ACC	31
2.13	SEM patterns of the cement paste samples	32
3.1	Cubic and cylindrical specimens after demoulding	38
3.2	Interlocking tile specimen	38
3.3	Water curing of specimens	40
3.4	Steam curing scheme	41
3.5	Steam curing chamber	42
3.6	Set up for carbonation curing chamber, and) Carbonation chamber used in this study	42
3.7	Compression testing of cubes and tiles	43
3.8	Water permeability test apparatus	46
3.9	Specimen covered with PVC film and conventional tape	47
3.10	Schematic diagram of water permeability test apparatus	47
3.11	Scanning electron microscope	49
4.1	Compressive strength test results at the ages of 3,7 and 28-days of casting	51
4.2	Compressive strength development rate of different curing regimes	53
4.3	Porosity test results at the ages of 3, 7 and 28-days of casting	54
4.4	: Relationship between compressive strength and porosity	57
4.5	Permeability test results at the ages of 3,7 and 28-days of casting	58
4.6	Mass loss curve of ACC cured specimens	60
4.7	XRD analysis of different curing regimes after 3 days of casting	60
4.8	XRD analysis of different curing regimes after 28 days of casting	61
4.9	SEM analysis of four different curing regimes at the age of 3-days of casting	63

4.10	SEM analysis of four different curing regimes at the age of 28-days of casting	64
4.11	Interlocking tile specimen (a) Dimensions (b) After demoulding	65
4.12	Compressive strength test results at the ages of 3, 7 and 28-days of casting	66
4.13	Porosity test results at the ages of 3, 7 and 28-days of casting	67

Abbreviations

ACC	Accelerated carbonation curing
WC	Water curing
SC	Steam curing
CC	Calcium carbonate
CH	Calcium hydroxide
C₃S	Tri-calcium silicate
C₂S	Di-calcium silicate
PC	Parvious concrete
RH	Relative humidity
OPC	Ordinary Portland cement
CKD	Cement klin dust
GA	Recycled fine glass aggregate
RCA	Recycled coarse aggregate
NA	Natural aggregate
C-6	Specimen cured adopting ACC for 6 hours
C-12	Specimen cured adopting ACC for 12 hours

CHAPTER 1 - INTRODUCTION

1.1 GENERAL

For the concrete to develop desired properties over time, it is essential to maintain the adequate moisture content within a favourable temperature range, required for hydration reaction in concrete. This is achieved by curing of concrete. Curing should begin as soon as possible after placing and finishing of concrete. Reasonable curing duration as per relevant standards is required for the concrete to achieve its potential strength and durability. Curing is more important in the early ages of concrete to meet the requirement of service. It is of utmost importance to start curing immediately within an hour or two after pouring concrete to prevent cracks. For proper curing, the temperature should be well maintained as the relative humidity and the rate of hydration of cement are greatly influenced by the temperature.



Figure 1.1: Curing of concrete

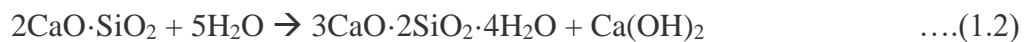
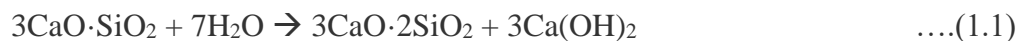
Curing can be done in the following ways:

- By covering the concrete with an impermeable membrane which helps in preventing an excessive loss of moisture from the concrete.

- By continuously wetting the surface with water to provide sufficient moisture content for curing.

In general, curing of concrete is done until it attains the target strength. Duration of curing of concrete depends on the number of factors such as material properties of concrete's ingredients, mix design, target strength, the geometry of concrete member, temperature and exposure conditions. Depending on these factors, duration may vary from a few days to a month or more. IS 456:2000 provides guidelines for the duration of curing (*"www.nbmcw.com"*).

Hydration process starts immediately after the mixing of water with ingredients of concrete. Calcium silicate hydrate (C-S-H) is the product of the reaction between water and cement constituents, which provides strength to concrete. Following reaction takes place between cement and water during the hydration process



Hydration product C-S-H gel binds the aggregates of concrete resulting in the formation of rock-solid mass and enhances strength and durability properties of concrete. Curing assists continuation of cement hydration reaction and formation of C-S-H gel; thus, further improving strength and durability properties of concrete.

1.2 COMMONLY USED CURING TECHNIQUES

The type of curing and its age is generally decided based on working procedure and weather condition of the site. Some basic curing techniques that are widely followed around the world are discussed below, along with their advantages and disadvantages.

1.2.1 Water curing

Water curing being the most commonly used method, is also an efficient and economical method of curing. In this method, water is directly applied to a concrete member by sprinkling or ponding method.

(a) Sprinkling method

Continuous or periodically sprinkling of water is a widely adopted method of curing. When sprinkling of water is done at intervals, it should be ensured that concrete should not become

dry between intervals of applications of water. This prevents the possibility of cracking caused by alternate cycles of wetting and drying of concrete. The sprinkling of water can be done either using a pipe or water can be applied using a system of nozzles. Demerits of this method are its cost, requirement of a considerable supply of water and careful supervision (["www.ccanz.org.nz"](http://www.ccanz.org.nz)).



Figure 1.2: Water curing by sprinkling method

(b) Ponding method

It is a popular and widely used curing technique. In this method, concrete is cured by storing water on a horizontal surface. A Canvas is used to cover the exposed surface of the concrete after the concrete is placed. This canvas is removed after 24 hours, and clay or sand is used to create small ponds to store water. These ponds are then further divided into rectangles, and then the water is filled in the ponds. Ponds are refilled with water twice or thrice in a day.

- Advantages of ponding method.
 1. Better than other methods under most curing conditions.
 2. Horizontal surfaces can be easily cured by using this method.
 3. No skilled labour is required.
- Disadvantages of ponding method.
 1. Cannot be used for vertical surfaces.
 2. Requires high amounts of water.
 3. Difficult to clean after curing is finished.



Figure 1.3: Curing of the concrete slab by ponding method

1.2.2 Membrane curing

In this method, a waterproof membrane is used to cover the concrete surface to prevent the water from evaporating. This type of curing takes about a week. Plastic sheet, bitumen emulsion, water-resistant bitumen paper, and wax emulsion are used as a membrane in this method. Concrete strength gain in this method is lesser as compared to other concrete water curing methods (["www.ccanz.org.nz"](http://www.ccanz.org.nz)).

Sheet curing technique might not be so efficient but generally provides acceptable results for all types of works except for special works, and it is more convenient to carry out curing using sheets as compared to other curing methods for vertical as well as horizontal surfaces.

- Advantages of membrane curing.
 1. Reduced evaporation.
 2. Can be easily adopted for vertical and horizontal surfaces.
 3. Weathering of concrete is prevented.
- Disadvantages of membrane curing.
 1. Strength of concrete is reduced.
 2. The initial cost is high as wax emulsion, bitumen emulsion, etc. are used.

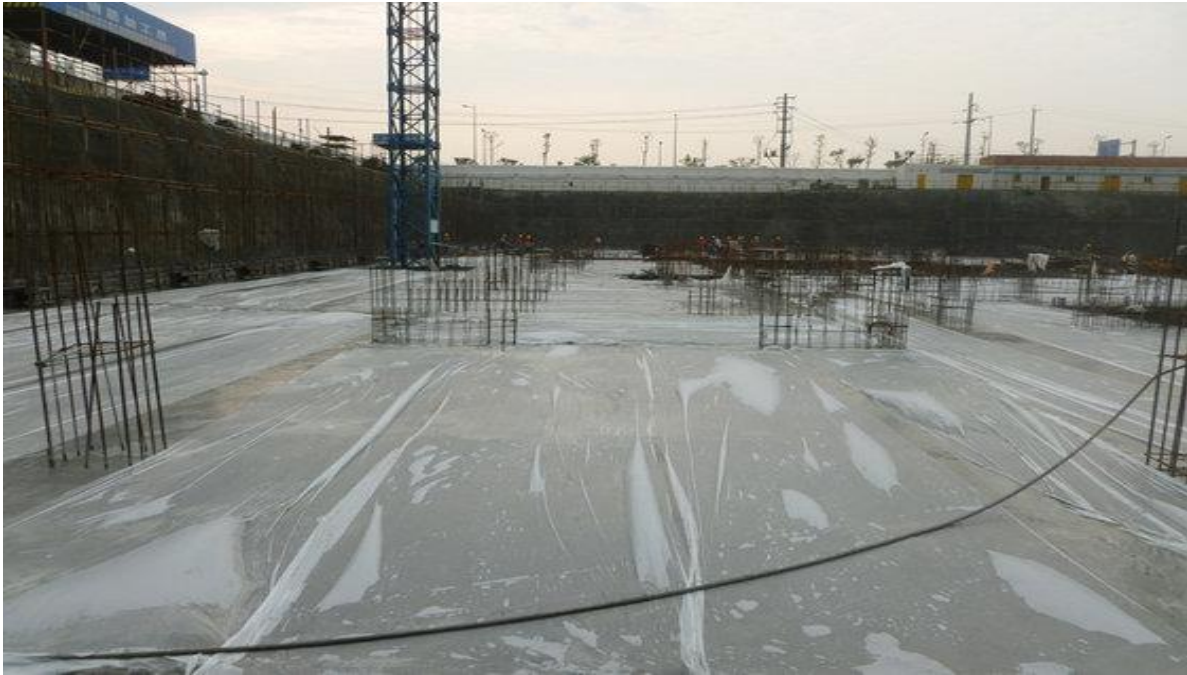


Figure 1.4: Membrane curing

1.2.3 Steam curing

Steam curing is the commonly employed curing method for precast concrete products. In this method, due to high curing temperatures, strength gain of concrete is very rapid. The temperature is generally kept below 75°C as a proper humidity level is required to prevent the concrete from drying. Temperature can be raised to 100°C in case of hot water curing.

Steam curing involves exposure to warm steam during hardening of concrete and mortar. Steam curing develops high early strength by speeding up the rate of hydration reactions. In steam curing, objects to be cured are put inside a chamber or room. Using a control panel, an operator can set the temperature and humidity level. Depending upon device capabilities pressure may also be varied. The warm steam penetrates the materials quickly to hydrate and hardens them. Steam curing requires a fraction of the time involved in comparison to traditional curing and rapidly strengthens the products so they can be used immediately.

The steam curing procedure consists of five stages. First is the delay period followed by the second stage of the period of gradual increase in temperature. The third stage is maintaining a constant maximum temperature. The fourth is the period of the gradual decrease in temperature followed by the fifth stage of the cooling period.

Stage –I

Steam curing takes place at high temperatures. This can induce tensile stresses within concrete due to the combination of thermal stresses induced by higher temperatures in the concrete and the pressure exerted by water in the pores of concrete at higher temperatures.

Steam curing process initiated immediately after casting of concrete will lead to the formation of cracks due to tensile stresses induced by steam curing. As concrete has not gained much strength by that time of casting, it cannot withstand tensile stresses. Formed micro-cracks led to the delayed formation of ettringite, which upon its formation later induces expansion and results in further weakening of concrete. *Alexanderson, 1972; Mironov, 1966* concluded that the delay period should be determined in such a way that the steam curing operation should not cause expansions. Therefore, a delay period is allowed to elapse before the commencement of the steam curing process to allow the concrete to gain a certain minimum tensile strength to resist tensile stresses induced by steam curing. *Alexanderson, 1972* observed that the delay periods of 4–7 h results in no strength loss at later ages.

The setting time of the concrete is an important criterion to determine the delay period. Generally, the delay period is kept equal to the initial setting time, which has been found to give satisfactory results. Compressive strength of steam-cured concrete increases with increase in delay period has been reported in earlier literature (*Hanson, 1963*).

Stage II and IV

In order to avoid the development of temperature gradient which adversely affects the concrete, between outer and inner portions of concrete, gradual rate of increase and decrease of temperature should be adopted (*Hernández-Bautista et al., 2017*). Development of temperature gradient between outer and inner portions of concrete results non-uniform hydration of concrete cross-section. This results in an earlier and higher degree of hydration of the outer part compared to the inner portion of concrete.

A gradual change in temperature during stage II and IV avoids rapid changes in volumes due to the sudden increase in hydration products in case rapid changes in temperature, which causes cracks in the concrete. During the high rate of temperature increase and decrease, the concrete temperature lags behind that of the steam curing chamber due to the time needed for the heat transfer to and from the inner portions of concrete respectively. Therefore, if the steam

application starts before the setting time of the concrete, the outer portions of a concrete specimen harden earlier while the inner concrete is still plastic. This results in a rigid hardened shell formed around the inner plastic concrete. As the internal temperature increases due to steam application and heat of hydration, the inner plastic concrete will try to expand. Therefore, the exterior rigid shell can be damaged due to the tensile stresses induced by this expansion.

Rapid lowering of steam curing chamber temperature results in a reduction of temperature in outer parts of concrete. For inner parts, heat transfer takes time and a higher temperature is still maintained for inner parts. This causes contraction of the outer portion of concrete while inner portions at high temperature remain intact, which results in the formation of cracks. A gradual decrease in temperature is required to prevent sudden contraction, which can cause cracking.

Stage III

Stage three being the most essential part of steam curing involves curing of concrete at a constant maximum temperature known as curing temperature for certain pre-decided duration known as steaming period. Increase in the steaming period at curing temperature of 50 °C from 1 hour to 14 hours improved compressive strength and further increase in duration to 24 hours lead to a decrease in compressive strength has been reported, this indicates that there exists an optimum steaming period for steam curing depending on curing temperature (*Ba et al., 2010*).

It is also necessary to avoid concrete temperatures above 70 °C, as higher temperatures inhibit the formation of ettringite. At a later age, a hardened concrete previously exposed to higher temperatures may lead to delayed ettringite formation. That results in the growing ettringite crystals which exert pressure on the surrounding cement paste causing it to crack. Temperatures above 70 °C also lead to peeling of concrete cover, micro-cracks and non-uniform distribution of hydration products due to the high rate of hydration at elevated temperatures. As the curing temperature of steam curing increases later age strength decreases as compared to standard curing, due to increases in the deleterious effect of steam curing at on concrete at elevated temperatures. As suggested by researcher's optimum curing temperature of 60 °C for a steaming period of 8 hours lead to higher 28-day strength compared to standard curing has been adopted in this study (*Deogekar et al., 2013*).

Stage V

The cooling period is the duration for which steam cured specimens are kept room temperature

after the gradual decrease in temperature to room temperature. The cooling period is necessary because at the end of the fourth stage of steam curing chamber attains room temperature, but concrete takes time to transfer heat to surrounding and reduce its temperature especially inner portion of concrete needs more time to reduce its temperature to room temperature.



Figure1.5: Steam curing chamber

- Advantages of steam curing
 1. It requires less curing time as compared to other techniques.
 2. It is a better curing method in cold weather.
 3. This method is advantageous in precast concrete, as high early strength can be achieved.
- Disadvantages of steam curing
 1. The high initial cost of this curing method.
 2. Steam curing method will not be efficient for a large surface.
 3. Skilled labours are required.
 4. Special equipments are required.

1.2.4 Accelerated carbonation curing

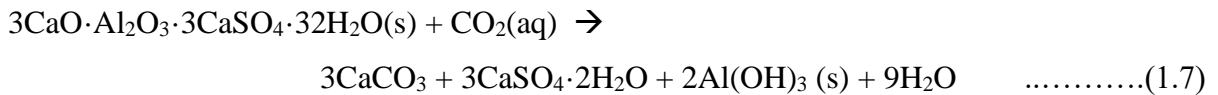
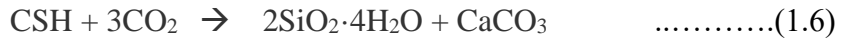
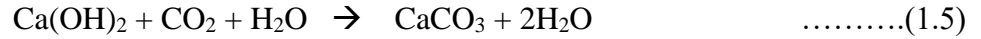
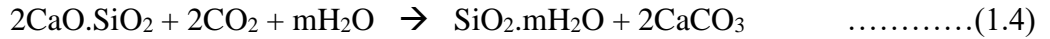
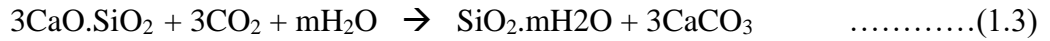
Climate change and global warming are the critical problems which today's world is facing and are affecting the environment severely. Carbon dioxide is a major cause of these problems.

The intensity of global warming and climate change are estimated to increase over the 21st century due to the projected increase in the amount of heat-trapping gases (e.g. CO₂, CH₄, N₂O) over the century. Therefore, today's world needs a reduction in CO₂ emissions as well as capture, storage, and consumption of already existing CO₂ to reduce its adverse effects on the environment.

One of the possible uses of CO₂ is through accelerated carbonation curing (ACC). Cementitious compounds are known for their ability to react with atmospheric CO₂. The carbonation reaction of the concrete takes place at a higher rate than hydration and provides accelerated growth. Carbonation also increases rate of hydration through precipitation of CaCO₃ which acts as a nucleation point for hydration of tri-calcium silicate. Depending upon parameters such duration of curing, pressure and temperature of CO₂, and material properties of ingredients of concrete or mortar accelerated carbonation curing can lead to an improvement in mechanical and durability properties of concrete. Consumption of greenhouse gas CO₂ during ACC is another aspect that attracts researchers towards ACC.

1.2.4.1 Mechanism and benefits of accelerated carbonation curing of concrete

Accelerated carbonation curing of the concrete is a process through which carbon dioxide sequestration takes place into precast concrete products during their fabrication. The CO₂ passed over concrete during ACC reacts with calcium compounds in cement and hydration products resulting in the formation of calcium carbonate and CSH gel as shown in equations (1.3-1.7), CaCO₃ is a stable compound with higher density and better mechanical properties than conventional hydration products. The calcium carbonate formed during ACC gets intermingled with C-S-H gel produced during the initial hydration of cement resulting in the formation of calcium-silicate-hydro-carbonate, which has better gel structure as compared to gel structure provided by conventional C-S-H gel produced during the reaction of cement with water. Products of the reaction of CO₂ with tri-calcium silicate, di-calcium silicate, calcium aluminate mono-sulfate, calcium aluminate tri sulfate, calcium hydroxide and CSH results in an increase in solid volume by 92.4, 108.6, 11.6, 23.15, 44.8, and 31.8 percent respectively (*Ahmad, 2018*). Carbonation products are more stable and have higher density, solid volume and denser microstructure than conventional hydration products, leading to improved mechanical and durability properties of concrete (*Rostami et al., 2012*). The chemical reactions take place during carbonation curing regime are as follows (*Shao and Monkman, 2006*).



Accelerated carbonation curing can reduce the pH of concrete by lowering the amount of calcium hydroxide due to the conversion of calcium hydroxide to calcium carbonate. In spite of the reduction in calcium hydroxide content, the value of pH remains well above the threshold value of 10, required for sustaining passive layer over reinforcements in RCC (*Rostami et al., 2012*). Reduced amount of calcium hydroxide is beneficial in increasing acid and sulphate resistance of ACC cured concrete (*Rostami et al., 2012, 2011*). Hence ACC can be used as a curing method for production for plain and reinforced, precast concrete products.

1.2.4.2 LABORATORY PROCESS OF CARBONATION CURING:

The following three-phase process is generally followed in the accelerated carbonation of concrete.

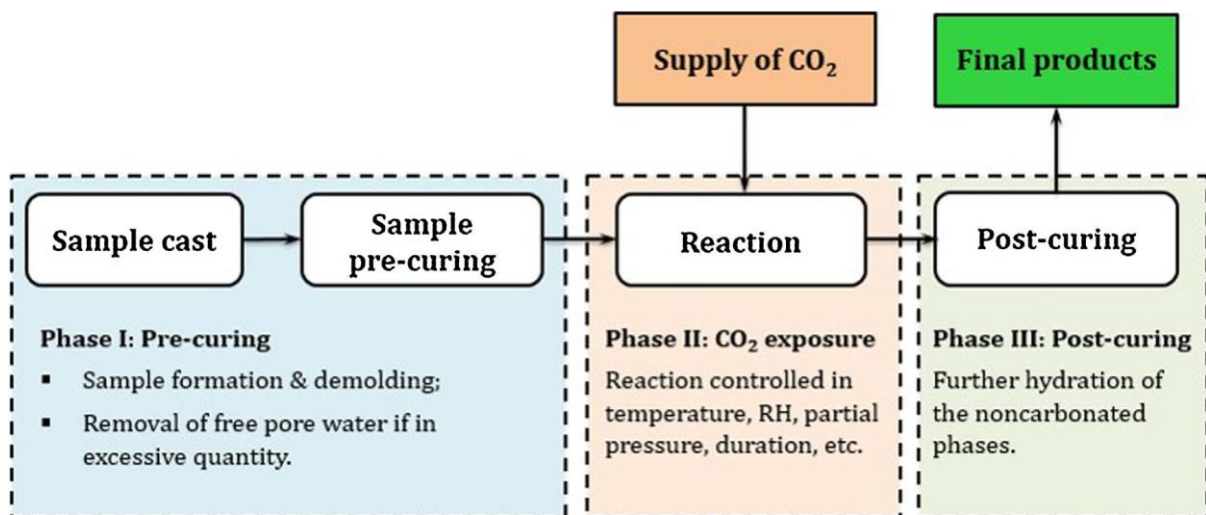


Figure 1.6: Laboratory process of carbonation curing (*Zhang et al., 2017*)

Phase I: Pre-curing

This process involves the controlled removal of water from the surface of the specimen after it has been de-moulded. This is an important step for the effective carbonation to occur as the majority of the reaction takes place in the presence of water and presence of the optimum amount of water needs to be ensured for the effective carbonation. Presence of excess water can cause blocking of reactants from CO₂ while water depletion can result in an incomplete reaction.

Phase II: CO₂ exposure

CO₂ curing can be done under two systems: enclosed and flow-able. Enclosed systems are generally used for the process as they have higher reaction efficiencies and can store CO₂ under elevated partial pressures. To speed up the diffusion process pure CO₂ is generally used. The carbonation curing of Portland cement-based materials is usually done at a temperature of 20-25°C. The relative humidity is generally adopted in the range of 60-70%.

Phase III: Post-curing

Post-curing is done to provide sufficient moisture for the continuation of hydration reaction at later ages. For the post-curing, any of curing process mentioned in section 1.2 can be adopted. The depletion of water due to pre-curing and carbonation curing should be recompensed to make sure the proper hydration of the pervious concrete at the subsequent ages. In this study water immersion of specimens for 3-days following ACC is adopted.

- Advantages of ACC
 1. Improved mechanical and durability properties.
 2. It requires lesser curing time as compared to other techniques.
 3. This method is advantageous in precast concrete, as high early strength can be achieved.
 4. Water consumption is reduced, therefore can be used in water-scarce areas.
- Disadvantages of ACC
 1. High initial and maintenance cost as special equipment are required.
 2. ACC method will not be efficient for a large surface.
 3. Skilled workers are required

1.3.PERVIOUS CONCRETE



Figure 1.7: Pervious concrete pavement

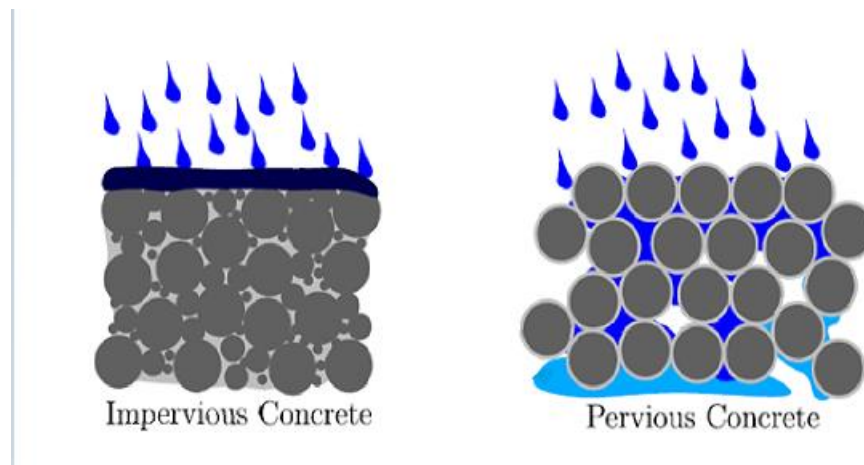


Figure 1.8: Drainage of water through pervious concrete (Zhong et al., 2018)

1.3.1 General

Pervious concrete, also known as no fines /permeable /porous concrete is a type of concrete with or without fine aggregate in it and is generally a mixture of cement, coarse aggregate and water. Chemical admixtures and cementitious materials can also be added to enhance physical properties.

Cement amount added should be sufficient to ensure coating of coarse aggregates with cement paste. Coarse aggregates can be of a single size or well graded. Pervious concrete has very low or zero content of fine aggregate, which leads to high porosity as well as a significant volume of interconnected voids and allows water to pass through it. Hence generally used in pavement applications to allow rainwater to pass directly through it, which causes a reduction in surface

run-off and recharges groundwater as water drains finally to groundwater from underlying soils.

Unlike conventional concrete for which its im-permeability is an important parameter, pervious concrete's quality is determined by its hydraulic conductivity. Constant water head is the most commonly used methods to assess the permeability of pervious concrete experimentally. Tortuosity plays a vital role in determining the permeability of pervious concrete. Tortuosity is defined as the square of the ratio of the average flow path length L_e to the length L , along the major flow axis of the pervious medium.

Pervious concrete has stiff consistency, as indicated by its zero slump value. Compaction of pervious concrete can be done with tamping, vibration or by use of proctor hammer. Compaction should take care of desired mechanical strength without neglecting permeability property, which strongly depends on its porosity. Compressive strength of pervious concrete depends on strength of binder paste, aggregate and porosity. Compressive strength of pervious concrete can be increased by increasing compaction effort, the addition of a small amount of fine aggregate, polymers and non-metallic fibers, and addition of supplementary cementitious materials (*Sonebi et al., 2016*).

Lower mechanical properties are the major disadvantage of pervious concrete. With compressive strength generally varying between 2.7- 29 MPa, pervious concrete has limited application as a pavement material for high volume traffic highways but can be used for parking lots, parks, sidewalks and low volume traffic roads. The porosity of pervious concrete generally varies from 15 to 35% by volume. Porosity between 15 and 25 % has been reported to provide adequate strength and permeability.

1.3.2 Advantages of pervious concrete.

Pervious concrete has many advantages such as it reduces volume and pollution of run-off water, flood risk, need for storm water infrastructure, heat island effect and road salt application, recharges groundwater, improves pavement noise absorption performance, and eliminate pollution generating from asphalt pavements and sealers (*Zhong et al., 2018*). Most essential advantages are discussed below.

1. The foremost advantage of pervious concrete is its good drainage properties. Pervious concrete prevents pooling of water on pavement surfaces and improves groundwater

quality of soil beneath. Pervious concrete is also used as shoulders along with conventional pavement owing to its drainage properties.

2. Pervious concrete has higher noise absorption properties because of its high porosity. In comparison to other pavement surfaces such as concrete and asphalt, noise generated by the traffic on the pavement is lesser for pervious concrete pavement, due to this pervious concrete pavement is regarded as “quiet” surface course (*Barišić et al., 2017*).
3. Pervious concrete pavements help in reducing the urban heat-island effect. Pervious concrete pavements due to its open structure do not absorb and store heat and then radiate it back into the environment like a typical asphalt surface, which causes heat island effect.
4. Pervious concrete uses 50-65% of aggregate as compared to 60-75% aggregate used in conventional concrete. Hence, pervious concrete leads to the preservation of natural aggregate. Pervious concrete is addressed as an environment-friendly material by EPA of united states (*Barišić et al., 2017*).

1.4 SCOPE OF THE PRESENT WORK.

The aim of this study is to find ways to enhance the performance and production of pervious concrete. Present work attempts to study the effects of different curing regimes on pervious concrete. Traditional water curing, steam curing, and accelerated carbonation curing are adopted as curing regimes. Effects of different curing regimes have been compared, in terms of their impact on compressive strength, porosity, and permeability. Microstructure and morphology of cured pervious concrete are also examined using SEM, TGA and XRD analysis to understand changes occurred in strength and durability properties and products formed from curing processes.

CHAPTER 2 - LITERATURE REVIEW

2.1 GENERAL

With the increase in world population, there is an ever-growing need for infrastructure for various purposes (industry, housing projects, dams etc.), which in turn utilises vast quantity of concrete. Cement being the most essential ingredient of concrete is consumed in huge quantity in production of concrete and cement production is associated with emission of greenhouse gases, which puts considerable pressure on environment. According to various figures huge number of researchers have shown their interest in the field of production of sustainable material. Pervious concrete is regarded as sustainable material. Accelerated carbonation curing causes consumption of greenhouse gas CO₂. The way researchers utilised ACC in various thrust areas are being discussed in the below section and highlighting the importance of each research carried out in this regard.

2.2 COMPRESSIVE STRENGTH

Guo et al., 2018 used natural fine aggregate (S) and recycled fine glass aggregate (GA) as fine aggregate, and ordinary portland cement (OPC) strength class 52.5R as a binding material to make the architectural mortar. GA was used as a 100% replacement of S. C/A was kept constant at 1:3. For natural aggregate mortar, water to cement ratio was 0.51, and for recycled glass aggregate mortar water to cement ratio was increased to 0.54 to improve workability.

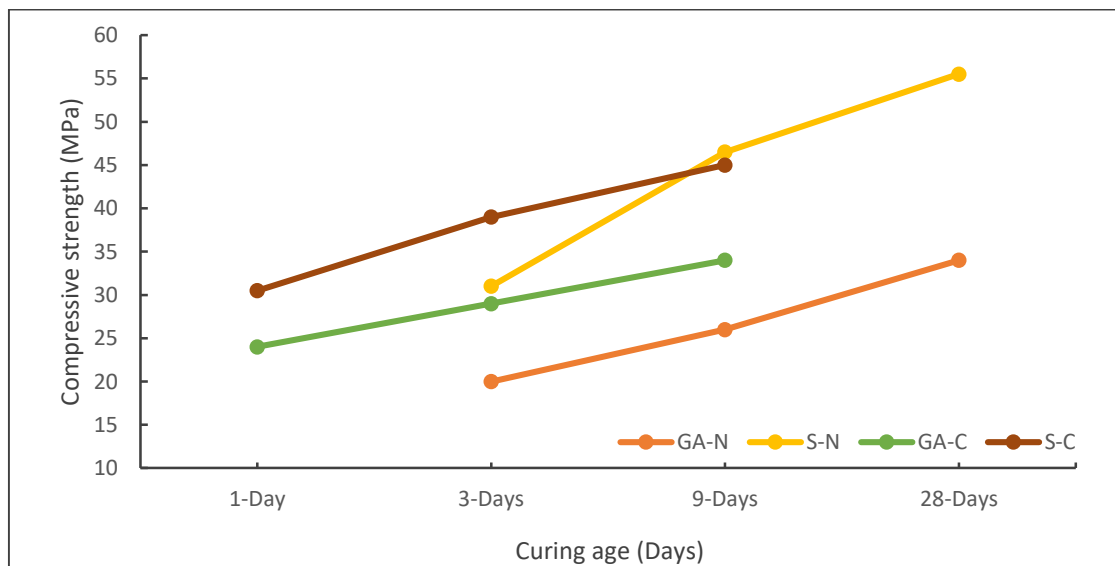


Figure 2.1: Effect of RG on the compressive strength of water and CO₂-cured mortars at different ages (*Guo et al., 2018*)

Gain in compressive strength with curing age, of water cured samples (S-N and GA-N), and ACC cured samples (S-C and GA-C) was reported as presented in Figure 2.1. GA water cured samples (GA-N) has compressive strength 37, 42, and 37 % lesser than natural aggregate water cured samples (S-N) counterparts at the age of 3, 9 and 28-days, respectively. ACC cured natural aggregate samples (S-C), and recycled glass aggregates samples (GA-C) have shown significant improvement in compressive strength compared to their water cured counterparts at 3, 9, and 28-days. After 3-day curing compressive strengths of S-C and GA-C were 123 and 149.2 % respectively of their water cured counterparts were reported.

Ahmad et al., 2017 studied the effect of pressure and duration of accelerated carbonation curing (ACC) on the compressive strength of concrete. Type I cement, fine quartz sand and crushed limestone of maximum size 12 mm were used as binding material, fine aggregate and coarse aggregate respectively, for preparation of concrete. Accelerated carbonation curing at different pressures (10,20,30,40,50 and 60 psi) and duration (1 to 10 hours) was used for curing concrete. Results presented in Figure 2.2 shows that compressive strength of concrete increases with increase in duration of ACC, and variations with an increase in pressure in compressive strength were marginal. Authors concluded that duration has control on the enhancement of compressive strength through ACC, rather than ACC pressure level.

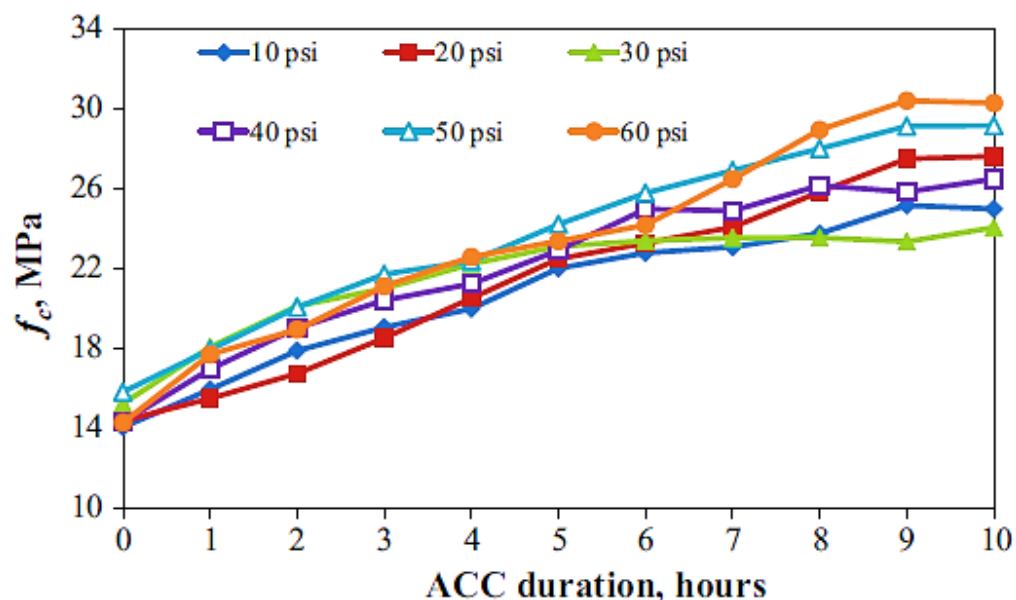


Figure 2.2: Compressive strength of concrete at different pressures and durations of ACC (*Ahmad et al., 2017*)

He et al., 2016 studied the compressive strength of concrete which has been subject to water curing till testing age after it has been cured by ACC for 3 hours. OPC, river sand and gravel (5-10mm) as binding material, fine and coarse aggregate respectively, were used for making the concrete. Two types of curing regime were followed. Samples were cured either cured for 5 hours in the air and after that water curing till testing age (Group A) or for 3 hour ACC was done and after that water curing till testing age (Group B, C, and D). Group B, C, and D had residual W/C ratio 0.11, 0.18 and 0.25, respectively. Group A showed the highest strength at 90 days, with 9.1 MPa higher compressive strength than ACC cured samples. Authors reported that amongst the samples that had undergone CO₂ curing, the compressive strength of all the specimens increased with the increase of water curing time, which indicated that further hydration of uncarbonated cement occurred. Group C had higher compressive strength at all ages as compared to Group B and D, and authors attributed this to the optimum moisture content in case of group C. Higher moisture content than optimum results in blocking of CO₂ penetration and lower moisture content than optimum reduces the efficiency of CO₂ curing, as moisture required for CO₂ curing.

Mo et al., 2017 studied the effects of concrete made with steel slag as binding materials as well as fine aggregate (<5 mm) and coarse aggregate (5-16 mm). Mix proportions were as given in Table 2.1. Moist curing and accelerated carbonation curing (ACC) were employed as curing regimes. Moist cured samples shown relatively lower compressive strength as compared to ACC cured samples regardless of aggregate type. Authors reported compressive strength of all the samples increased significantly after exposer to ACC for 1-day, as shown in Table 2.2. Compressive strength concrete specimens subjected to 14 days ACC, demonstrated an increase of 4.2-5.2 times in compressive strength as compared to moist cured counterparts. Authors attributed this to the formation of carbonate products during ACC.

Table 2.1: Mix proportion of different mixes (*Mo et al., 2017*)

Mix design	Binding materials				Fine aggregates	Coarse aggregates
	Steel slag	Portland cement	Reactive magnesia	Lime		
SCM-S	60	20	20	0	Steel slag	Steel slag
SCLM-S	60	20	10	10	Steel slag	Steel slag
SCM-N	60	20	20	0	Sands	Limestone
SCLM-N	60	20	10	10	Sands	Limestone

Table 2.2: Compressive strength of moist cured and CO₂ cured specimens (Mo et al., 2017)

Mix design	Moist curing	CO ₂ curing			
	28d	Before carbonation (moist cured for 7d)	1d	3d	14d
SCM-S	11.5	10.7	38.6	52.7	61.3
SCLM-S	10.5	9.4	33.5	48.4	55.9
SCM-N	10.7	9.0	24.6	40.8	46.2
SCLM-N	9.4	7.9	27.6	36.6	41.2

Sharma and Goyal, 2018 studied the effect of accelerated carbonation curing (ACC) on compressive strength of mortars containing cement kiln dust (CKD) 0,5,10,20,30,40 and 50 % as a replacement of cement by weight. Specimens were cured through three different curing regimes. One set was cured through water curing (WC) till testing age, and set 2 (C) and set 3(CS) were cured with ACC for 12 hours. Set 3(CS) was water cured for three days after ACC and sealed in plastic bags till testing age. While set 2(C) was sealed in plastic bags after 12 hours ACC till testing age. Three-day test results show the highest compressive strength for CS followed by C and lowest strength was attained by WC counterparts. Authors attributed this to the formation of CaCO₃ in carbonation specimens C and CS, which due to its higher density and volume, densifies the microstructure. Which results in higher compressive strength of C and CS specimens. 28-day Compressive strength was highest for CS followed by WC and lowest for Authors credited this to the formation of additional CSH during further water curing of CS specimens for three days.

Grubeša et al., 2018 studied compressive strength capability of single size pervious concrete aggregate using six different mixtures. Table 2.3 shows mix proportions of six different mixtures. Six mixtures were fabricated using 10 % river sand as fine aggregate and three different coarse aggregates steel slag, dolomite, and diabase, with two different sizes, 4-8 mm and 8-16 mm. Samples were subjected to water curing till testing age of 28 days of casting. Dolomite mixtures achieved higher compressive strength when 4-8mm size aggregates were used in pervious concrete preparation while steel slag and diabase samples achieved higher compressive strength when higher size 8-16 mm were used in pervious concrete preparation. Table 2.3 shows the compressive strength achieved by different mixtures.

Table 2.3: Characteristics of different mixtures of pervious concrete (*Grubeša et al., 2018*)

Characteristics	C1	C2	C3	C4	C5	C6
Compressive strength [MPa]	21.1	25.04	10.87	15.57	10.31	15.8
Water/cement ratio	0.33	0.33	0.33	0.33	0.33	0.33
Sand 0–2 mm [kg]	178.4	178.4	178.4	178.4	178.4	178.4
Dolomite 4–8 mm [kg]	1605.3	-	-	-	-	-
Dolomite 8–16 mm [kg]	-	1605.3	-	-	-	-
Diabase 4–8 mm [kg]	-	-	1687.7	-	-	-
Diabase 8–11 mm [kg]	-	-	-	1687.7	-	-
Steel slag 4–8 mm [kg]	-	-	-	-	1848	-
Steel slag 8–16 mm [kg]	-	-	-	-	-	1848

Xu et al., 2017 used commercially available fly ash and OPC as cementitious materials, crushed limestone and diabase as coarse aggregates of size 2.36 to 26.5 mm, and calcareous sand as fine aggregate (FA) of size 0.06 to 4.75 mm for making of pervious concrete (PC). Mixture PC-FA (15% fine aggregate) has reported an increase in compressive strength of 5.2 and 2.8 % at 7 and 28 days respectively than mixture PC-1 (without fine aggregate), which is due to presence 15% fine aggregates in PC-FA. Mixtures with fly ash and fine aggregate content reported 30 to 48 % higher compressive strength compared to samples made only with coarse aggregates at each curing time. Results indicate that fly ash has improved the compressive strength of pervious concrete significantly. Addition of fine aggregates and fly ash increases the contact area among coarse aggregates, which results in an increase in compressive strength of pervious concrete.

Yap et al., 2018 studied the properties of pervious concrete containing blended natural coarse aggregate (NA) and recycled coarse aggregate (RCA). For the making of pervious concrete OPC, natural and recycled coarse aggregates of size 4.5 to 9.4 mm were used. Six mixtures were prepared by replacing 0, 20, 40, 60, 80 and 100 % NA with RCA. All the RCA mixes had shown lower 28-days compressive strength as compared to NA specimen. The trend of a decrease in compressive strength with increase in RCA replacement has been reported. Compressive strength development with a curing age of 0 to 28 days was as shown in Figure 2.3.

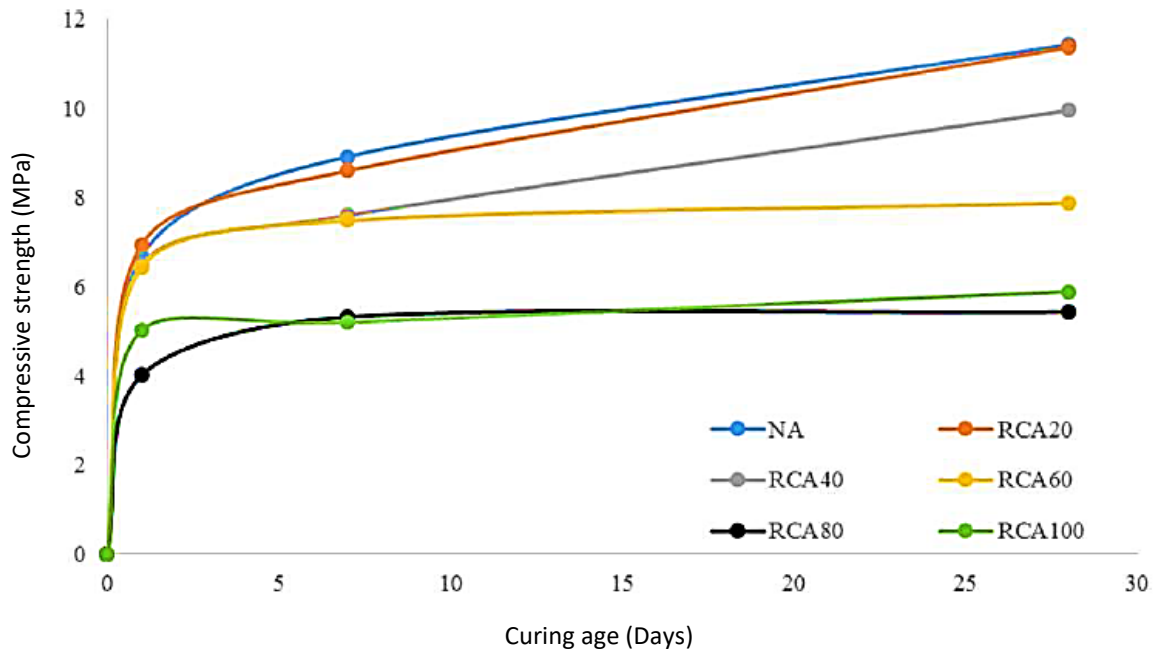


Figure 2.3: Compressive strength development with curing age (Yap et al., 2018)

Shen et al., 2017 studied the effects of steam curing on concrete containing metakaolin (MK). Four mixes were prepared. C-0 control mix made with OPC, quartz sand and crushed limestone as fine and coarse aggregates (5-10 mm) respectively. C1, C2, and C3 had metakaolin 5, 10 and 15% as a replacement of cement. Steam curing was performed at 80 C for a period of 8 hours. On steam curing compressive strength of specimens increased with increase in metakaolin content up to 10% and on further increase in MK content to 15% slight decrease was observed in compressive strength. Authors reported that among the mixes highest compressive strength for standard curing was at 5% MK content whereas for steam curing it was at 10%.

Ba et al., 2011 studied the effect of steam curing on the compressive strength of concrete with a low water/cement ratio. Water cement ratio was kept at 0.30. Fly ash was used for replacement of cement, 30% by weight of cement. Two curing regimes were followed. Group 1 was steam cured at different durations and then stored in lime saturated water till testing age, and Group 2 was subjected only to lime saturated water. Compressive strength test results showed that Group 1 has higher Compressive strength than Group 2 samples. This can be due to steam curing, due to which hydration and pozzolanic reactions would have extended. Results of compressive strength tests indicated that the duration of steam curing affects the compressive strength of concrete. With an increase in steam curing duration from 0 to 14 hours, compressive strength also increased because with the increase in steam curing duration amount

of CSH gel increases. With further increase in steam curing duration beyond 14 hours to 24 hours compressive strength has shown a decline in value with increasing duration of steam curing, this occurs because steam curing coarsened the matrix which resulted in a decrease in compressive strength.

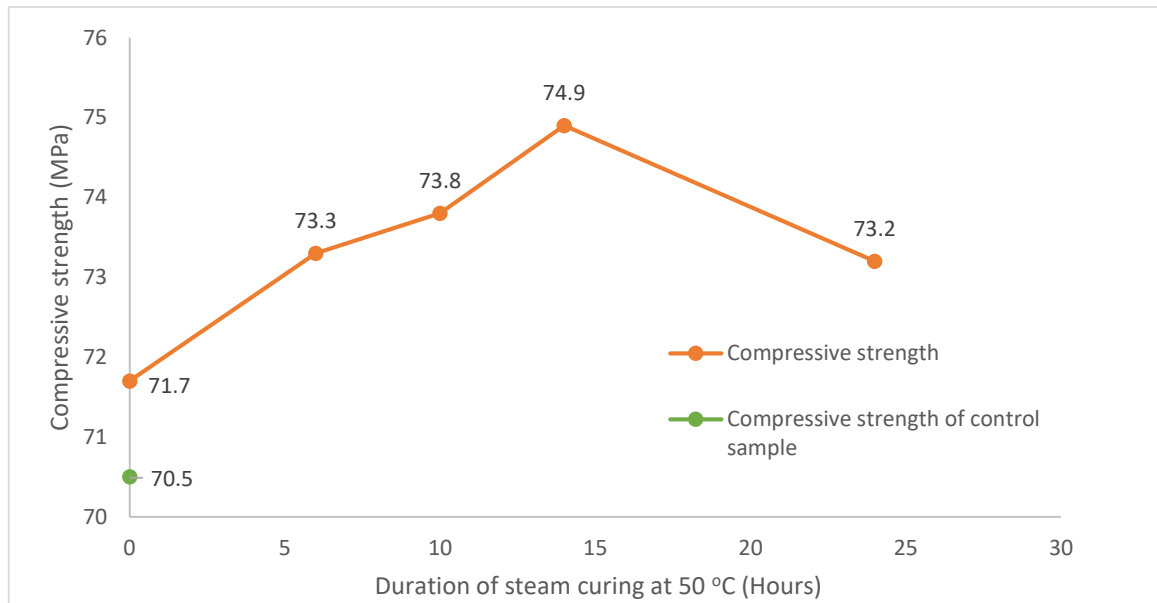


Figure 2.4: Effect of duration of initial steam curing at 50 °C (Ba et al., 2011)

2.3 Porosity

Sharma and Goyal, 2018 studied the effect of ACC on porosity of mortars containing cement kiln dust (CKD) 0,5,10,20,30,40 and 50 % as a replacement of cement by weight. Specimens were cured through three different curing regimes. One set was cured through water curing till testing age and set 2 and 3 were cured with ACC for 12 hours. Set 3 was water cured for 3 days after ACC and sealed in plastic bags till testing age. While set 2 was sealed in plastic bags after 12 hours ACC till testing age. The study shows that up to a cement replacement of about 10% by CKD, there is no significant effect on porosity. With the increase in the percentage of CKD beyond 10%, the porosity increases. It can be attributed to the decrease in the amount of C-S-H gel because of the lesser cement content as compared to the control specimen, and hence, a porous microstructure is achieved. Because of this, the permeable porosity of the mortar increases with a higher percentage of CKD in the mix. The increase in chloride content of mixes with higher percentages of CKD also contributes to an increase in porosity. When the porosity values of the carbonation cured and water cured mixes are compared, the carbonation cured specimens exhibit lower porosity as compared to water cured specimens.

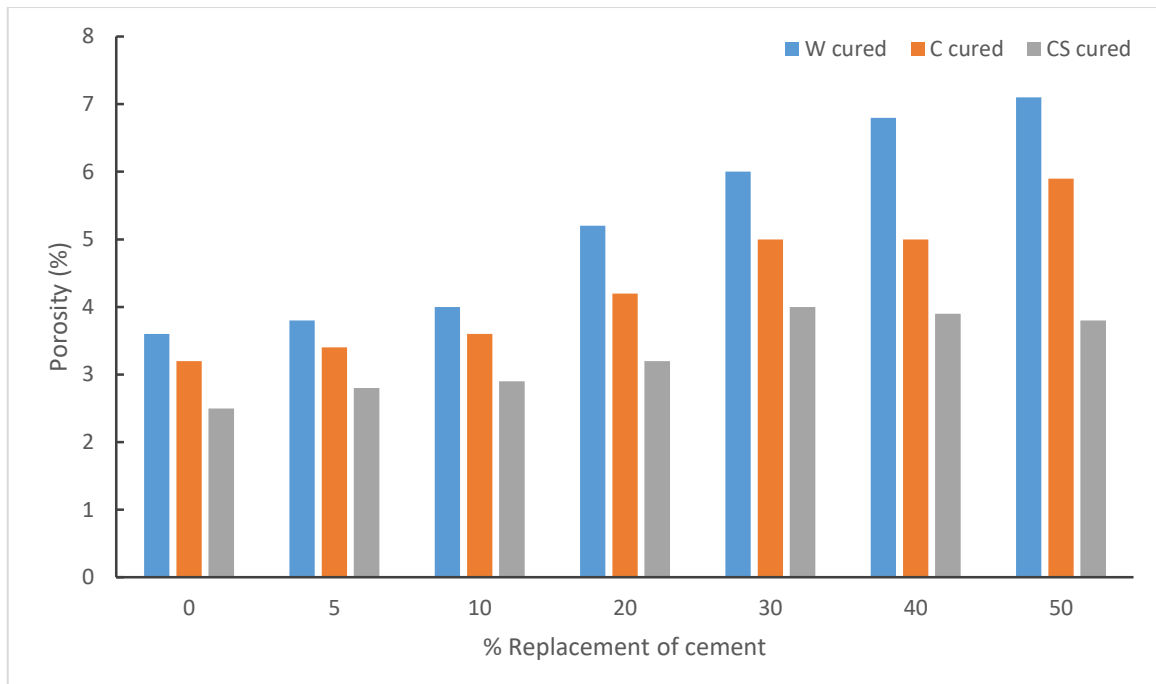


Figure 2.5: Comparison of porosity for water curing and carbonation curing for different percentages of CKD (Sharma and Goyal, 2018)

Guo et al., 2018 used natural fine aggregates (S) and recycled glass aggregates (GA) of maximum size 5 mm and OPC strength class 52.5R as cement to make the architectural mortar. GA was used as a 100% replacement of S. C/A was kept constant at 1:3. For natural aggregate mortar water to cement ratio was 0.51, and recycled glass aggregate mortar water to cement ratio was increased to 0.54 to improve workability. Addition of 100% GA slightly decreased the permeable voids. The decrease in the permeable voids can be attributed to the near-zero water absorption nature of GA. After 9 days of CO₂ curing, however, all the samples displayed much lower permeable voids. Permeable voids of ACC cured natural aggregate samples (S-C) were 8.2% lower than those of their water cured counterparts (S-N). Permeable voids of ACC cured GA sample (GA-C) were 37.8% lower than those of their water cured counterparts. This was likely due to the decrease in porosity and an increase in density induced by CO₂ curing. It is worth noting that GA-C had a higher decrease rate in permeable voids compared with S-C.

Grubeša et al., 2018 studied compressive strength capability of single size pervious concrete aggregate using six different mixtures. Six mixtures were fabricated using 10 % river sand as fine aggregate, three different coarse aggregates steel slag, dolomite and diabase and two different sizes, 4-8 mm and 8-16 mm. Samples were subjected to water curing till testing age of 28 days of casting. Mixtures made with dolomite C1 and C2, C2 reported higher porosity

due to the greater size of coarse aggregates. While in case of a mixture made with diabase (C3 and C4) and steel slag (C5 and C6) have shown the almost similar value of total porosity irrespective of the coarse aggregate size used.

Table 2.4: Characteristics of different mixtures of pervious concrete (Grubeša et al., 2018)

Characteristics	C1	C2	C3	C4	C5	C6
Total Porosity (%)	24	27	31	30	29	29
Water/cement ratio	0.33	0.33	0.33	0.33	0.33	0.33
Sand 0–2 mm [kg]	178.4	178.4	178.4	178.4	178.4	178.4
Dolomite 4–8 mm [%–kg]	1605.3	-	-	-	-	-
Dolomite 8–16 mm [kg]	-	1605.3	-	-	-	-
Diabase 4–8 mm [kg]	-	-	1687.7	-	-	-
Diabase 8–11 mm [kg]	-	-	-	1687.7	-	-
Steel slag 4–8 mm [kg]	-	-	-	-	1848	-
Steel slag 8–16 mm [kg]	-	-	-	-	-	1848

Yeih and Chang, 2019 studied the influences of cement type and curing conditions on pervious concrete containing electric arc furnace slag as a fine aggregate. Authors used four types of cement with different physical and chemical properties type 1, type 2, sulpho-aluminate cement and calcium aluminate cement. Two curing conditions were adopted; first curing condition was saturated lime water curing, and the second curing condition was air curing. Connected porosity results shows following sequence of connected porosity valve sulpho-aluminate cement (22.07%) > calcium aluminate cement (21.31 %) > type I cement (18.64%) > type II cement (16.41%). Above sequence was due to the volume of products during hydration (i) products of hydration of cement and (ii) other chemical reactions with formation of tri sulphate or ettringite. Excessive formation of tri sulphate or ettringite might have occurred for calcium aluminate cement and sulpho-aluminate cement, due to reaction with electric furnace slag. Expansion of tri sulphate or ettringite induces microcracks.

2.4 PERMEABILITY

Hanh et al., 2017 studied durability properties of pervious concrete containing seashells. Authors used cement 52.5R, coarse and fine aggregates of size 0-4mm and 2-6.3mm

respectively and three different types of seashells *Crepidula* (CRPC), scallop (SCPC) and queen scallop (QSPC). The permeability coefficients of pervious concrete with or without crushed shells varies between 2.2 and 3.4 mm/s; these values were greater than the recommended value of 1 mm/s. CPC represents control pervious concrete mix. PC represents pervious concrete in Figure 2.6.

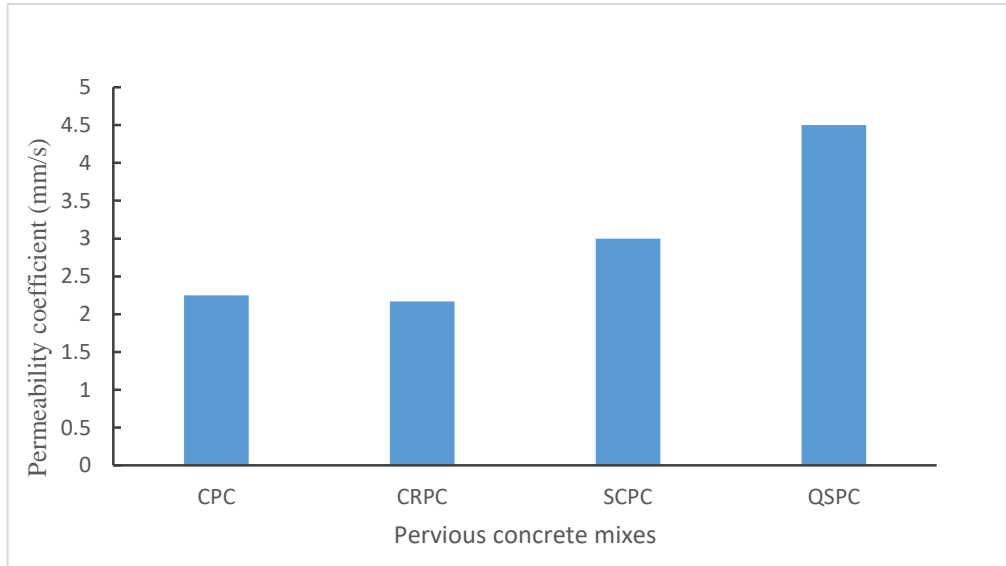


Figure 2.6: Permeability of different pervious concrete mixes (Hanh et al., 2017)

Yap et al., 2018 studied the properties of pervious concrete containing blended natural coarse aggregate (NA) and recycled coarse aggregate (RCA). For the making of pervious concrete OPC, natural and recycled coarse aggregates of size 4.5 to 9.4 mm were used. Six mixtures were prepared by replacing 0, 20, 40, 60, 80 and 100 % NA with RCA. The permeability coefficients of all the six mixes were in the range of 1.42 to 2.64 cm/s. For RCA 20 and RCA 40, permeability coefficients value was close to that of NA mix and with further increase in replacement of NA by RCA that is for RCA 60 samples permeability coefficients increases by 30-65 %. Table 2.5 shows the permeability coefficient value at a different replacement. The trend is because when the content of RCA was increased, the cement paste connected between the aggregates gets reduced as cement paste is utilised to form aggregate and cement paste bonding. With less available cement paste connecting between the aggregates, a larger porous network is available for the water to flow through the pervious concrete.

Table 2.5: Permeability properties of all mixes (Yap et al., 2018)

Mix	Permeability coefficient (cm/s)	%Increment/decrement relative to NA mix
NA	1.6	-
RCA20	1.42	-11%
RCA40	1.71	+7%
RCA60	2.11	+31%
RCA80	2.64	+65%
RCA100	2.38	+49%

Ramkrishnan et al., 2018 studied the influence of mineral admixtures on pervious concrete. Authors used OPC 53 grade cement, locally available coarse aggregates with bulk density 1900 kg/m³ and specific gravity 2.68. Metakaolin (M), fly ash (F), and ultra-fine ground granulated blast furnace slag (UFGGBFS) were used as a replacement of cement and a super-plasticiser to provide required flow to concrete. The following Table 2.6 shows permeability coefficient values obtained after replacement of cement by FA, M or U. First letter in Table 2.6 represents replacing materials and number next to it represents the percentage of cement replaced by material.

Table 2.6: Permeability of Various Mixes (Ramkrishnan et al., 2018)

Specimen	Permeability (cm/s)
Standard	0.97
U-10	1.05
M-10	0.81
M-15	0.79
M-20	0.72
F-10	1.77
F-15	1.32
F-20	1.19

Yeih and Chang, 2019 studied the influences of cement type and curing conditions on pervious concrete containing electric arc furnace slag as a fine aggregate. Authors used four types of cement with different physical and chemical properties type 1, type 2, sulpho-aluminate cement and calcium aluminate cement. Two curing conditions were adopted. First curing condition was saturated lime water curing and second curing condition was air curing. Value of permeability coefficients in descending order were calcium aluminate cement (0.762) > type I cement (0.681) > type II cement (0.452) under saturated water curing condition; and sulpho-aluminate cement (2.40) > calcium aluminate cement (0.80) > type I cement (0.70) > type II cement (0.69) for air curing condition. Connected pore volume was larger than expected because no compaction has been performed in this study. As different type of cement react differently with water and aggregates, so permeability due to these reaction's products was different for different types of cement. Sulpho-aluminate cement and calcium aluminate cement reacted with electric arc furnace slag, and the reaction product was tri-sulfate or ettringite, the expansion of tri-sulfate or ettringite resulted in lots of void and cracks inside pervious concrete such that they had higher permeability coefficient.

2.5 XRD ANALYSIS

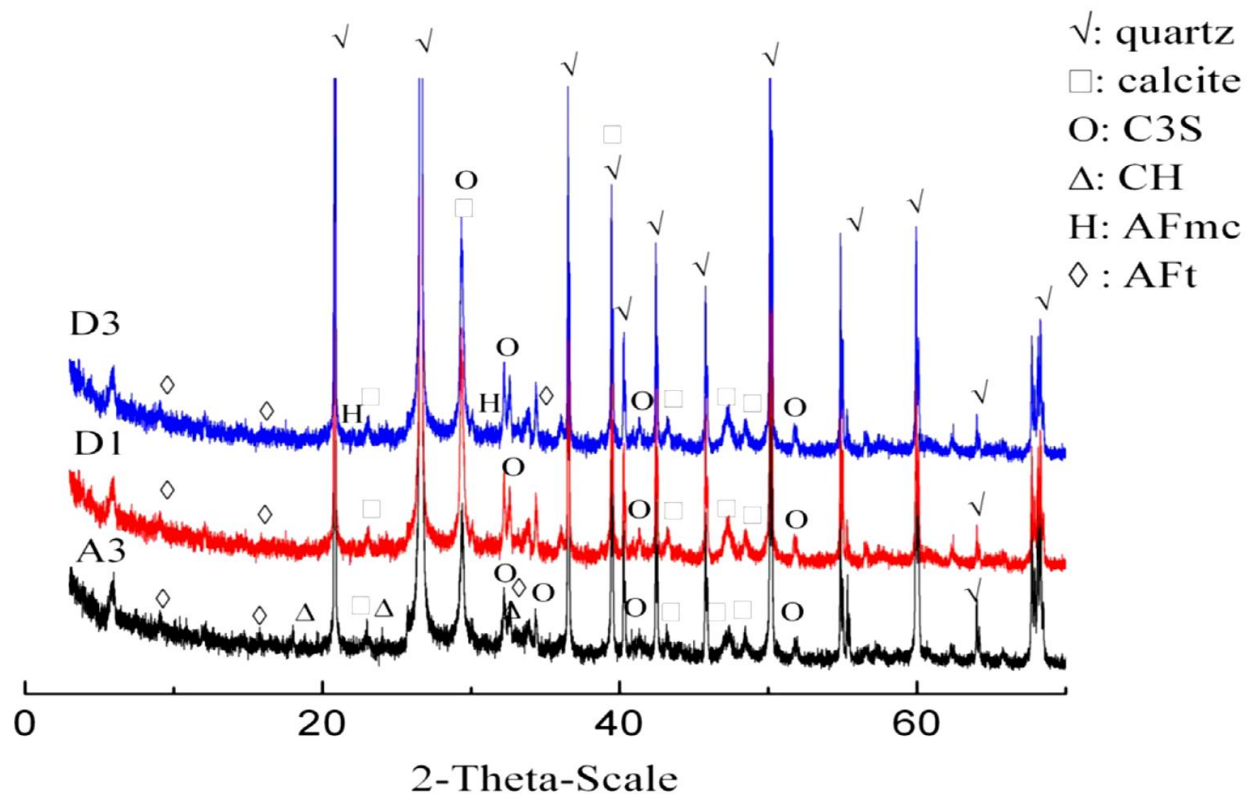


Figure 2.7: XRD results of cement mortars cured with different curing regimes (*He et al., 2016*)

He et al., 2016 studied the microstructure of concrete which has been subject to water curing till testing age after it has been cured by ACC for 3 hours. OPC, river sand and gravel (5-10mm) were used as fine and coarse aggregate respectively. Two types of curing regime were followed. Samples were cured either cured for 5 hours in the air and after that water curing till testing age or for 3 hour ACC was done and after that water curing till testing age. For microstructure analysis, mortar samples were prepared to eliminate the influence of coarse aggregates. XRD analysis revealed that phase changes occurred during further water curing, a new crystallised phase has been identified is calcium mono-carbon-aluminate hydrate, which is formed by the hydration of tri-calcium aluminate in the presence of calcium carbonate. The lack of calcium hydroxide peaks among ACC cured samples is also reported, which due to the conversion of calcium hydroxide to calcium carbonate by carbon dioxide.

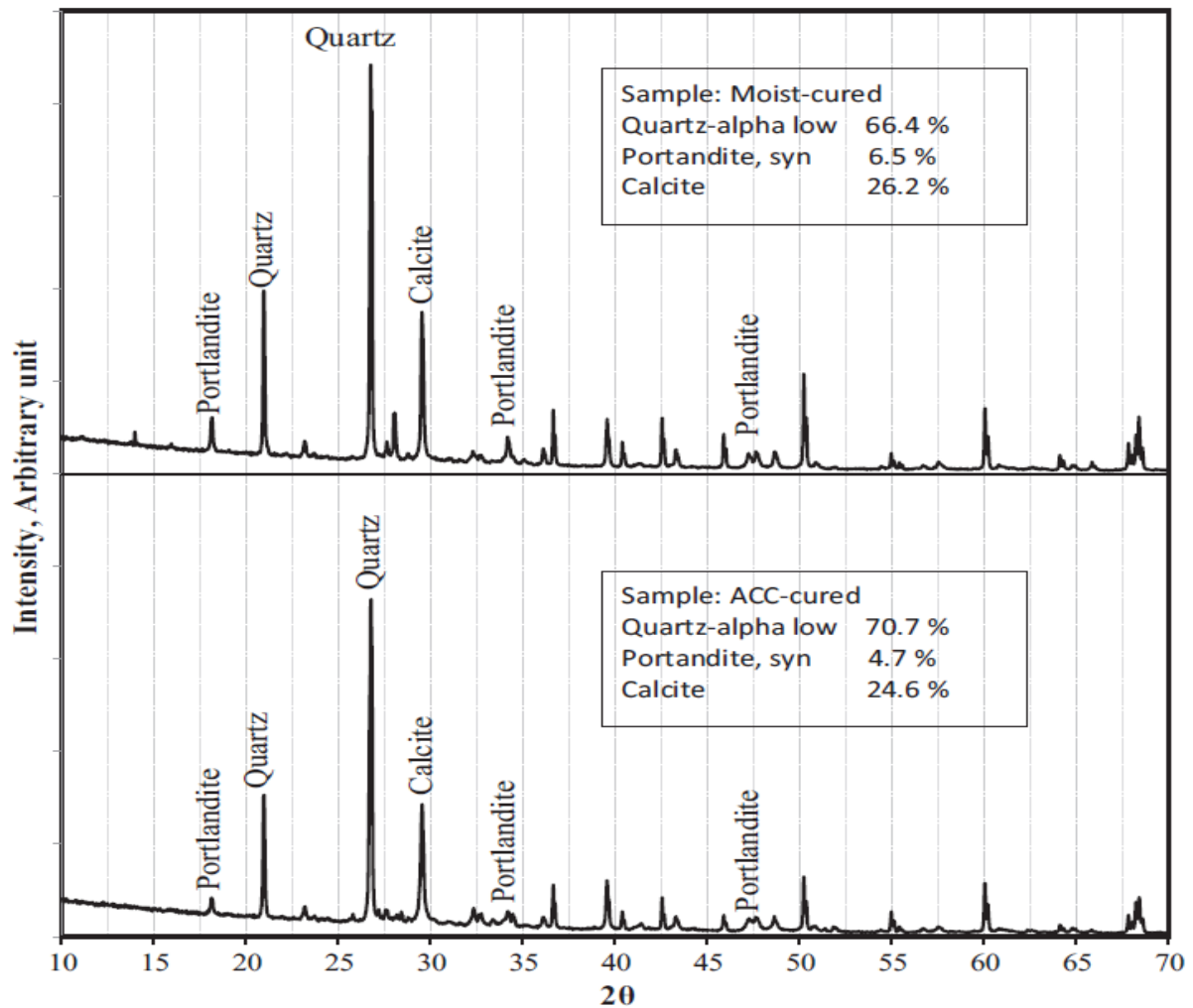


Figure 2.8: XRD results of moist and ACC cured concrete cured (*Ahmad et al., 2017*)

Ahmad et al., 2017 studied the effects of pressure and duration of ACC on concrete. Authors used type 1 cement as per ASTM, crushed limestone as coarse aggregate with maximum size 12 mm, dune sand as fine aggregate and to provide workability polycarboxylic based superplasticizer was added. Figure 2.8 provides phases of concrete samples subjected to moist curing and ACC, the formation of portlandite, calcite and quartz is noted in ACC-cured as well as moist- cured samples. Presence of portlandite is 28% lesser in ACC-cured samples compared to moist- cured counterparts, and this is due to the consumption of portlandite by carbon dioxide by converting portlandite to calcium carbonate.

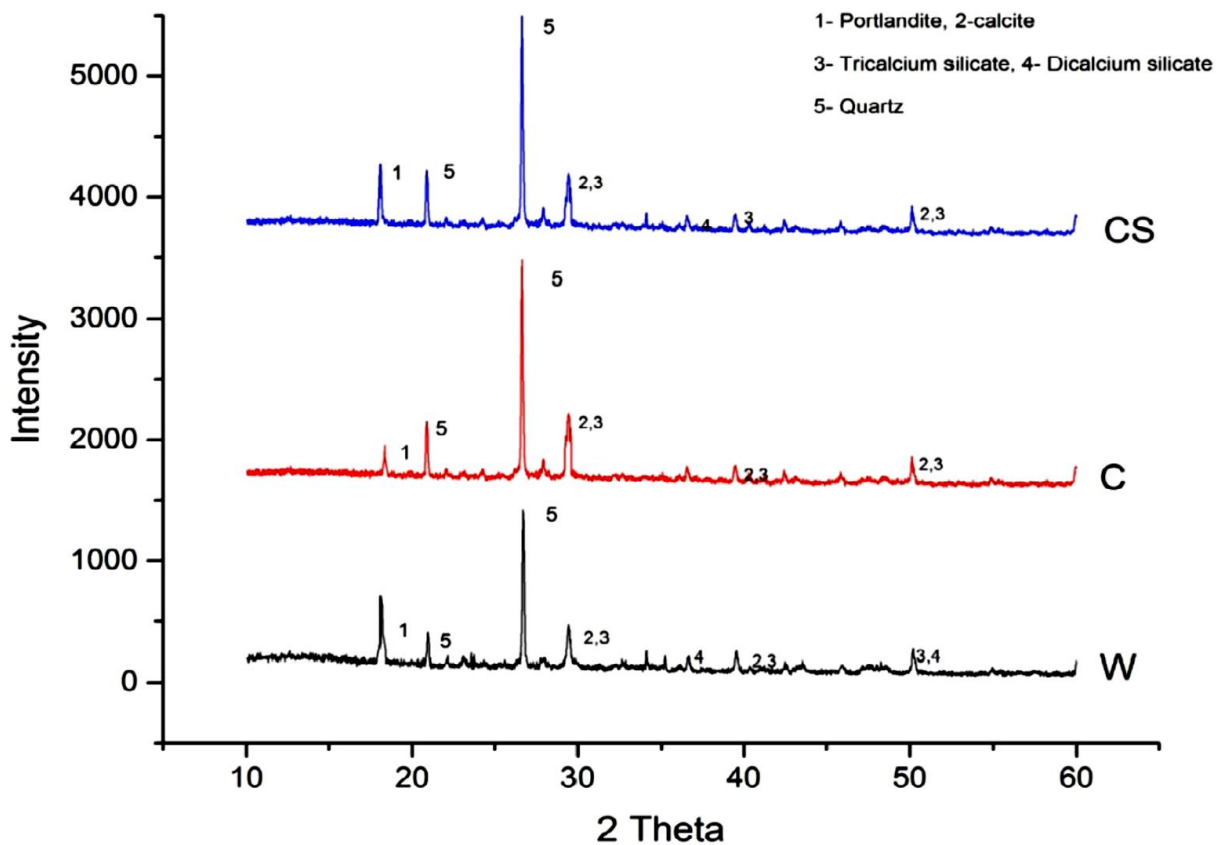


Figure 2.9: XRD analysis of different curing regimes after 3 days of casting (W- Water Cured, C-Carbonation Cured, CS-Carbonation curing followed by water spray)
(Sharma and Goyal, 2018)

Sharma and Goyal, 2018 studied the effect of ACC on porosity of mortars containing cement kiln dust (CKD) 0,5,10,20,30,40 and 50 % as replacement of cement by weight. Specimens were cured through three different curing regimes. One set was cured through water curing till

testing age and set 2 and 3 were cured with ACC for 12 hours. Set 3 was water cured for 3 days after ACC and sealed in plastic bags till testing age. While set 2 was sealed in plastic bags after 12 hours ACC till testing age. Results suggest strong peaks of calcite and reduced peaks of portlandite of ACC cured sample, which suggests the formation of calcite (CaCO_3) from portlandite upon carbonation by ACC. The peak of portlandite in CS-cured samples is stronger, which indicates significant hydration reaction due to water compensated by water spray which was lost during ACC as carbonation reactions are exothermic.

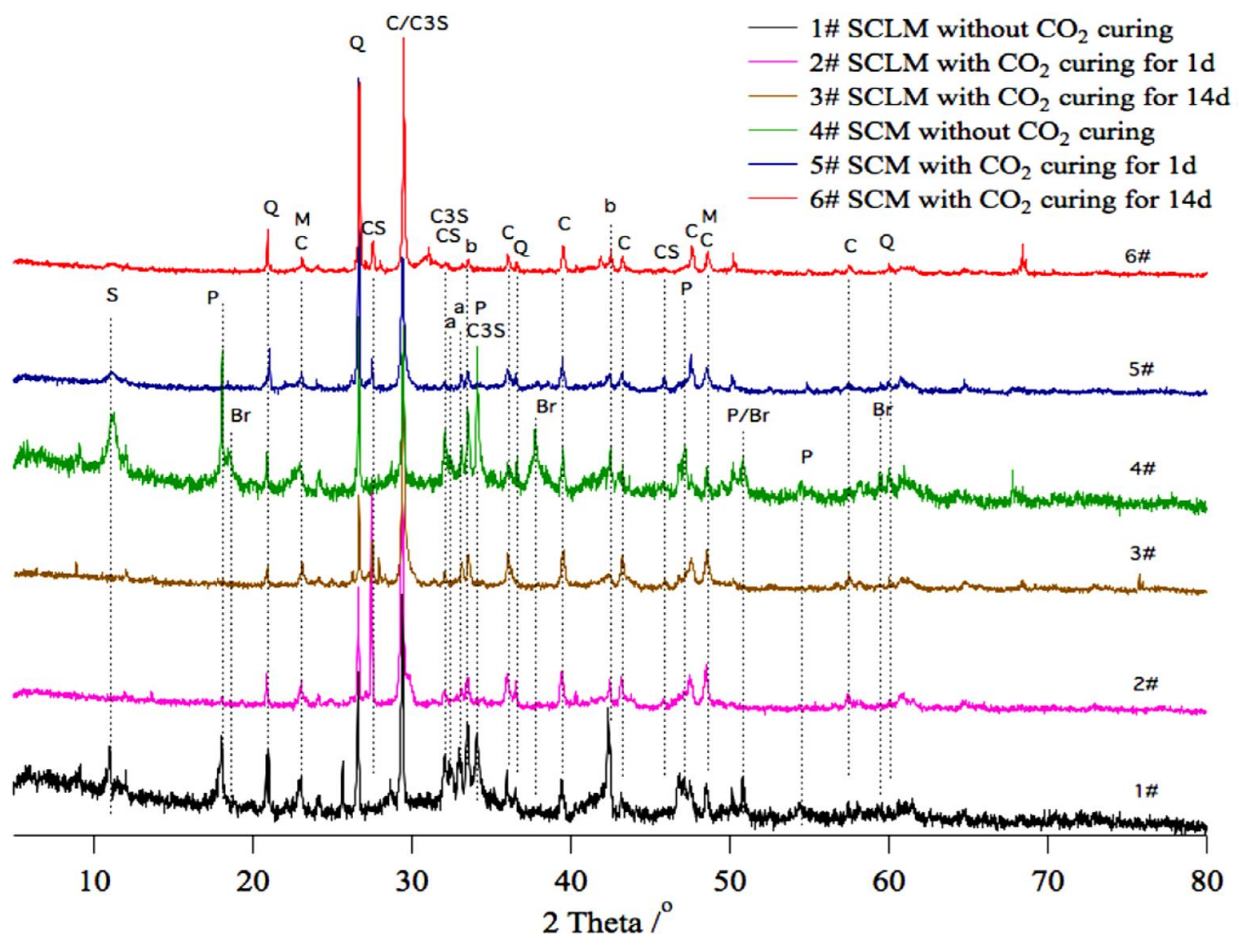
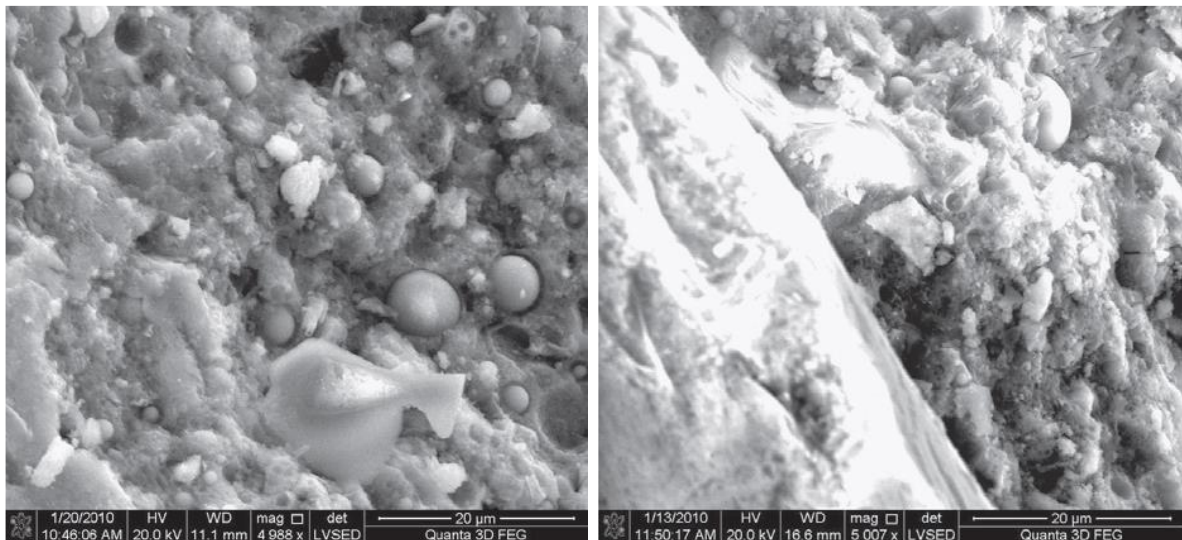


Figure 2.10: XRD patterns of moist and ACC cured samples (*Mo et al., 2017*)

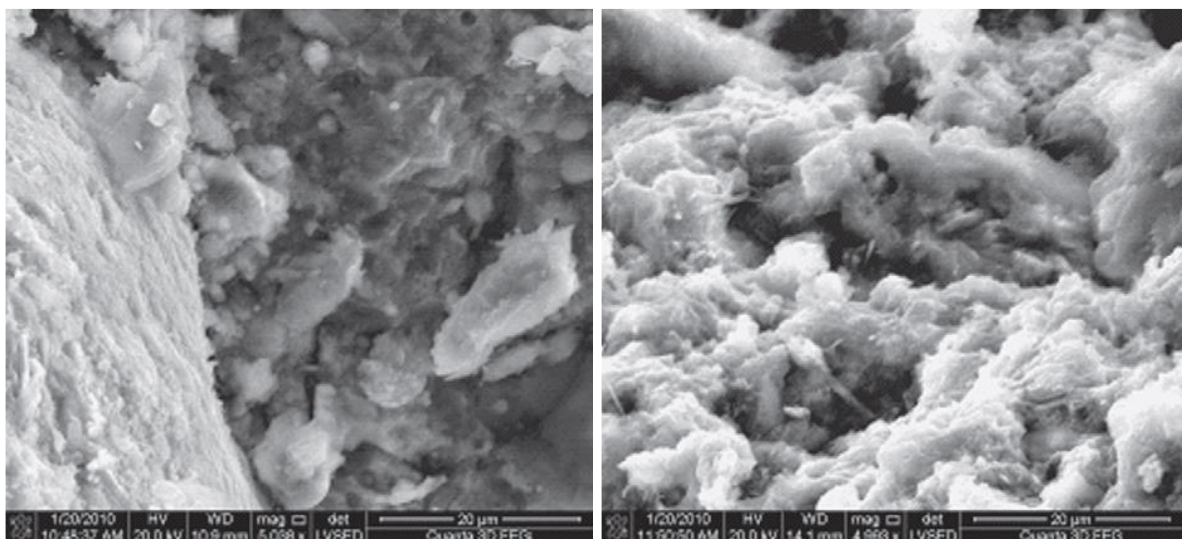
Mo et al., 2017 used moist and ACC as curing techniques for concrete. Portland cement type P II 52.5, lime, reactive magnesia, steel slag particles less than 5mm as fine aggregate and 5-16 mm as coarse aggregate were used for making of concrete. Notable peaks of Portlandite and brucite are observed in moist cured samples. Brucite is hydration product reactive magnesium oxide, and portlandite is due to hydration of cement, added lime and free calcium oxide present

in steel slag. For ACC cured concrete, the strong peak of calcite is observed due to the formation of calcite by the reaction between carbon dioxide with portlandite, brownmillerite and different calcium silicates present in cement and steel slag. The disappearance of peaks of Portlandite also confirms this.

2.6 SEM ANALYSIS



(a) 0-hours duration of steam curing (b) 5-hours duration of steam curing



(c) 14-hours duration of steam curing (d) 24-hours duration of steam curing

Figure 2.11: SEM micrograph of samples subjected to different duration of steam curing (*Ba et al., 2010*)

Ba et al., 2010 studied the microstructure of concrete subjected to steam curing having low W/C ratio. Cement and fly-ash were used as binding materials; cement was replaced by fly-ash 30% by mass .W/C was kept at 0.30. Two curing regimes were followed, group 1 was steam cured initially and then cured in lime saturated water till testing age and group 2 was subjected only to lime saturated water for curing till testing age. Authors had reported with increase in steam curing duration from 0 hours to 24 hours volume of fly-ash particles was reduced, and that of CSH gel increased as shown in Figure 2.11 (d), this suggests that degree of hydration of fly ash increased with increase in the duration of steam curing. For zero-hours steam curing samples fly-ash particles seen in Figure 2.11(a) were round and smooth and were embedded in pate.

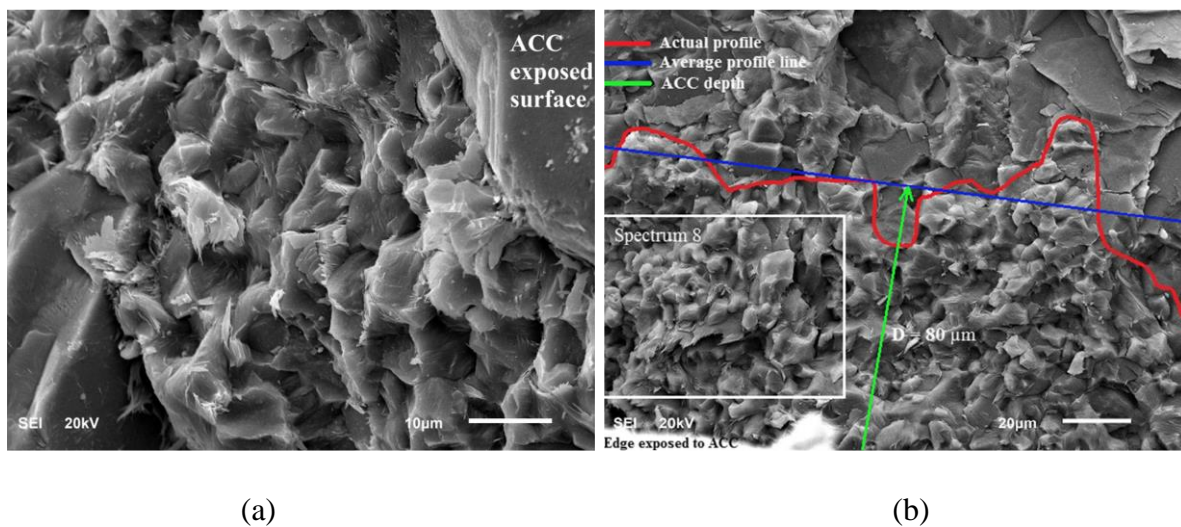


Figure 2.12: SEM micrograph of the specimen exposed to ACC (*Ahmad et al., 2017*)

Ahmad et al., 2017 studied the effects of pressure and duration of ACC on concrete. Authors used type 1 cement as per ASTM, crushed limestone as coarse aggregate with maximum size 12 mm, dune sand as fine aggregate and to provide workability polycarboxylic based superplasticizer was added. SEM analysis Figure 2.12(a) Shows that the formation of intermixed CaCO_3 -C-S-H due to the reaction of Carbon dioxide with Portlandite, calcium hydroxide, and conventional (C-S-H). This intermixing can be due to the fact that C-S-H will be highly porous after 18 hours of casting (i.e. when demoulding is done, and ACC commenced) as a result of the porous structure of C-S-H on commencing ACC diffusion of Carbon dioxide will occur, and portlandite will be converted to CaCO_3 by Carbon dioxide. Figure 2.12(b) shows a boundary between intermixed CaCO_3 -CS-H and continuous C-S-H. This is because intermixed CaCO_3 -C-S-H formed up to depth up to which Carbon dioxide has

reached, i.e. up to carbonation depth and at further depth (beyond boundary) Figure 2.12(b) only continuous C-S-H is available due to non-availability of Carbon dioxide.

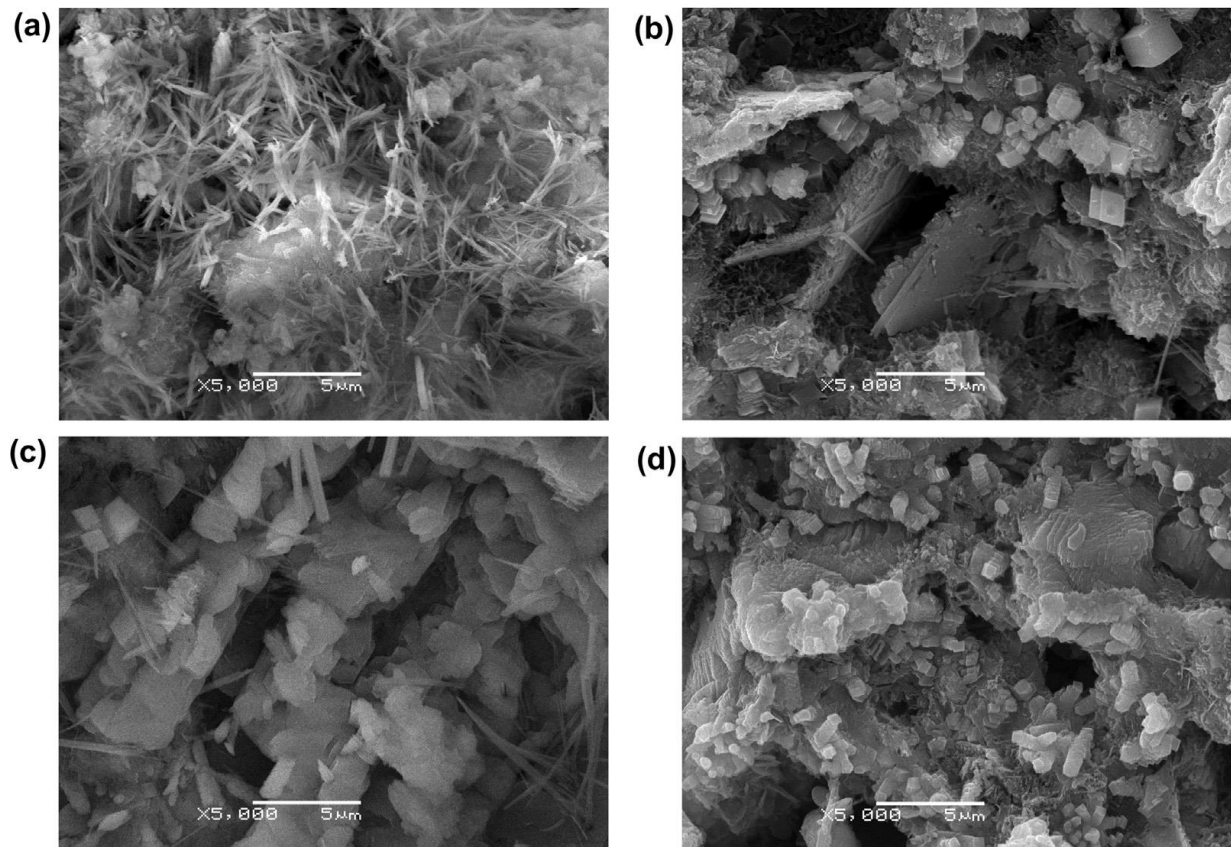


Figure 2.13: SEM patterns of the cement paste samples (Yan et al., 2018)

Yan et al., 2018 studied sulphate resistance of slag containing concrete subjected to steam curing (ST). Portland cement and slag were used as a binder (B), river sand and crushed stone of maximum size 20 mm was used for manufacturing the concrete. W/B ratio was kept at 0.5. Two curing regimes were used, standard and steam curing. SEM observation showed the presence of needle-shaped ettringite embedded in PC-ST specimens, as shown in Figure 2.13(a). In steam-treated (ST) specimens containing 20% slag (S20-ST) Figure 2.13(b) and 50% slag (S50-ST) Figure 2.13(c) shows the presence of needle-like ettringite as well as the tabular gypsum crystal. In steam-treated (ST) specimens containing 70% slag (S70-ST) specimen Figure 2.13(d) large quantity of gypsum is observed. Combined formation of gypsum and ettringite leads to deterioration of concrete on exposing to sulphate solution.

CHAPTER 3 - EXPERIMENTAL PROGRAM

This chapter describes in detail the properties of materials used in this study and experimental procedure followed to investigate strength properties (compressive strength) and durability properties (porosity and permeability) of pervious concrete mix. The chapter also describes in detail the various curing regimes used in this study and the methods (SEM, XRD and TGA) used to examine the microstructure of pervious concrete mix.

3.1 MATERIALS

Cement, coarse aggregate and water were used for the preparation of pervious concrete. The physical and chemical properties of these materials were investigated as per various standards. Following sections illustrate the specifications and properties of these materials.

3.1.1 Cement

In this study, Ordinary Portland Cement (OPC) of 43 grade was used. The chemical and physical properties of cement were tested in accordance with Indian Standard specifications (BIS 8112: 2013) and are shown in Table 3.1 and Table 3.2, respectively.

Table 3.1: Chemical properties of Ordinary Portland cement (OPC)

S. No.	Element	Compound (%)
1.	CO ₂	6.50
2.	Na ₂ O	1.42
3.	MgO	0.58
4.	Al ₂ O ₃	1.17
5.	SiO ₂	21.74
6.	SO ₃	6.11
7.	K ₂ O	2.85
8.	CaO	59.24
9.	FeO	0.39

Table 3.2: Physical properties of ordinary Portland cement (OPC)

S. No.	Characteristic	Obtained Result	Standard Values
1.	Fineness	3.5 %	Less than 10 %
2.	Specific Gravity	3.14	-
3.	Normal Consistency	30 %	-
4.	Initial Setting Time	150 min.	Should not be less than 30 min.
5.	Final Setting Time	385 min.	Should not be more than 600 min.

3.1.2 Coarse aggregates

The coarse aggregates used in this study were collected locally. Two types of coarse aggregate with a maximum aggregate size of 20 mm and 10 mm were used in a ratio of 60:40 by volume respectively (*Babu and Neeraja, 2017*), and the sieve analysis of the resultant mix of coarse aggregate was given in Table 3.6. Measurement of physical properties was done in accordance with BIS 383-2016; the values are shown in Table 3.3. The value obtained by the sieve analysis of coarse aggregate done in the laboratory for 20 mm is given in Table 3.4 and that for the 10 mm aggregate in Table 3.5.

Table 3.3: Physical properties of coarse aggregates

S. No	Characteristic	Values of 20 mm	Values of 10 mm
1.	Type	Crushed	Crushed
2.	Specific Gravity	2.70	2.69
3.	Fineness Modulus	6.93	6.10
4.	Total Water Absorption (%)	0.33	0.57

Table 3.4: Sieve size analysis of Coarse Aggregates (20mm)

IS sieve (mm)	Wt. retained (gm)	% age Wt. retained	Cumulative Wt. retained	Cumulative % age retained
40 mm	0	0	0	0
20 mm	160	3.20	160	3.20
10 mm	4410	88.20	4570	91.40
4.75 mm	360	7.20	4930	98.60
PAN	70	1.40	5000	100
$\Sigma=5000$				$\Sigma C = 193.20$
Fineness modulus = $\frac{\Sigma C + 500}{100} = (193.20 + 500) / 100 = 6.93$				
ΣC = Summation of Cumulative % age retained up to 4.75 mm				

Weight of sample taken = 5000 gm

Table 3.5: Sieve size analysis of coarse aggregates (10 mm)

IS sieve (mm)	Wt. retained (gm)	% age Wt. retained	Cumulative Wt. retained	Cumulative % age retained
40 mm	0	0	0	0
20 mm	0	0	0	0
10 mm	379	18.95	379	18.950
4.75 mm	1442.50	72.125	1821.50	91.075
PAN	178.50	8.925	2000	100
$\Sigma = 2000$				$\Sigma C = 110.025$
Fineness modulus = $\frac{\Sigma C + 500}{100} = (110.025 + 500) / 100 = 6.10$				
ΣC = Summation of Cumulative % age retained up to 4.75 mm				

Weight of the sample taken = 2000 gm

Table 3.6: Sieve size analysis of coarse aggregate (60% of largest size 20mm and 40% of largest size 10mm)

IS Sieve (mm)	Wt. Retained (gm)	%age weight retained	Cumulative Wt. retained	Cumulative %age Wt.
40	0	0	0	0
20	120	2.40	120	2.40
10	3516	70.32	3636	72.72
4.75	1198	23.96	4834	96.68
Pan	166	3.32	5000	100.00
$\Sigma = 5000$				$\Sigma C = 172.29$
Fineness modulus = $\frac{\Sigma C + 500}{100} = (172.29 + 500) / 100 = 6.72$ $\Sigma C =$ Summation of Cumulative % age retained up to 4.75 mm				

Weight of sample taken = 5000 gm

3.1.3 Water

In this experimental work, normal tap (potable) water of density 1000kg/ m³ was used for mixing of pervious concrete ingredients and for curing of samples. Water reacts with cement resulting in the formation of cement paste that acts as a binding agent. Generally, drinking water is suitable for concrete mixing. As per IS 3025-1984, the used potable water should be free from any type of heavy metal and other material such as organic matter, silt, petroleum, sugar, chloride and acidic matter that puts an unfavourable effect on the quality of concrete.

3.2 MIX PROPORTIONS

The strength and quality of the pervious concrete are generally associated with its compressive strength and permeability. As no standards are available for the design of pervious concrete mix, careful study of previous literature was carried out, and different trial mix proportions were selected to find mix with higher compressive strength. Eight trial mix were prepared with two different cement to aggregate ratios and four different water-cement ratios. The trial mixes were cast and cured under water curing regime and tested for 7-day compressive strength. Cement, coarse aggregate and tap water were used for the preparation of pervious concrete

mixes. Mix proportion, notations and compressive strength of trial mixes are shown in Table 3.7.

Table 3.7: Mix proportion and 7-day compressive strength of pervious concrete trial mixes

Mix	W/C	C/A	Cement (kg/m ³)	Coarse aggregate (kg/m ³)	Water (kg/m ³)	Compressive strength (MPa)
T-1	0.30	1:4	288	1233.60	86.40	6.93
T-2	0.35	1:4	288	1233.60	100.80	8.10
T-3	0.40	1:4	288	1233.60	115.20	7.24
T-4	0.45	1:4	288	1233.60	129.60	6.21
T-5	0.30	1:4.5	261.80	1261.64	78.60	6.25
T-6	0.35	1:4.5	261.80	1261.64	91.60	7.36
T-7	0.40	1:4.5	261.80	1261.64	104.70	7.68
T-8	0.45	1:4.5	261.80	1261.64	117.80	6.95

W/C - Water/cement ratio

C/A - Cement/aggregate ratio

Pervious concrete trial mix T-2 have achieved highest 7-day compressive strength among trial mixes. Therefore, mix proportions of trial mix T-2 with better strength properties were selected as a base mix for the present study.

3.3 CASTING

3.3.1 Casting

Four sets of specimens were cast as per the base mix. The nomenclature adopted for the representation of specimens under different curing conditions shown in Table 3.9. After mixing ingredients of pervious concrete thoroughly, cubic, interlocking tiles and cylindrical moulds were filled in three layers, and for each layer, compaction was done 25 times with standard tampering rod. Casted moulds were then kept at room temperature for a period of 18 hours.

After 18 hours of casting de-moulding of all the specimens was done, as shown in Figure 3.1, and then the specimens were subjected to subsequent curing procedures.



Figure 3.1: Cubic and cylindrical specimens after de-moulding

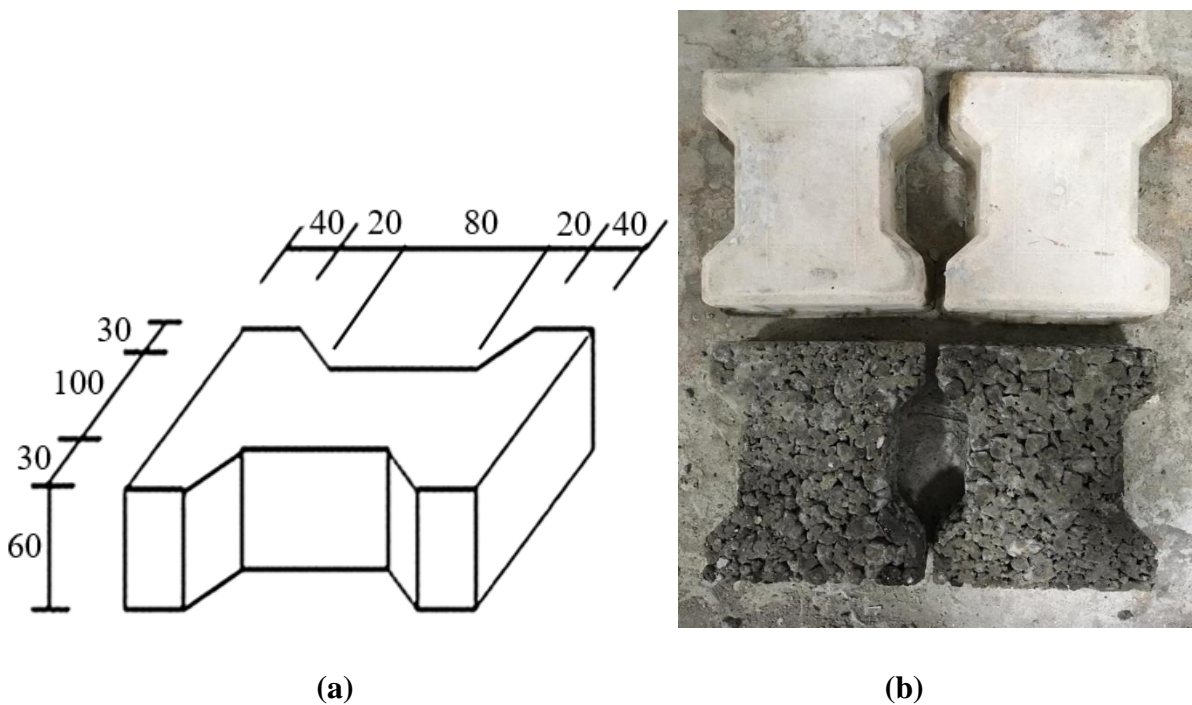


Figure 3.2: Interlocking tile specimen (a) Dimensions (b) After de-moulding

Table 3.8 Geometry of specimens used for testing different properties

Property	Specimen geometry	
	Shape	Size
Compressive strength	Cube	100 mm
	Tile section	60 mm Thickness
Porosity	Cube	100 mm
	Tile section	60 mm Thickness
Permeability	Cylinder	ϕ100 mm * 200 mm

3.4 CURING

In this present study, the effect of ACC on the properties of concrete was studied and compared with the corresponding steam and water curing procedures. For this, the specimens were divided into four categories. All the curing procedures were briefly discussed in the following sections.

The first set of specimens was cured through the conventional water curing while the second set and third set were cured through the accelerated carbonation curing for 6 and 12 hours respectively. The fourth set of specimens was cured by steam curing.

Table 3.9: The curing schemes and their designation

Curing scheme	Stages of curing (after de-moulding of the specimen at 18 hours of casting)				
	Pre-conditioning	Curing description	Post-conditioning	Subsequent curing	Set designat
Water curing	-	Water curing 27±2°C temperature and 100% RH	-	-	WC

Steam curing	Air drying at 30 °C (delay period) for a period of 4 hours	Steam curing - rate of change of temperature 10 C/hour, constant maximum temperature 60 C for 8 hours	Air drying at 30°C (cooling period) for 4 hours	Water curing till the age of testing	SC
Carbonation curing -I	Air drying at for a period of 4 hours	Carbonation curing for 6 hours	water curing for 3 days	Sealed in a plastic bag till age of testing	C-6
Carbonation curing- II	Air drying at for a period of 4 hours	Carbonation curing for 12 hours	water curing for 3 days	Sealed in a plastic bag till age of testing	C-12

3.4.1 Water curing

Water curing was done by immersing the specimens in water in the water tank at a temperature of $27\pm 2^{\circ}\text{C}$ and 100% RH till the testing age as shown in Figure 3.3.



Figure 3.3: Water curing of specimens

3.4.2 Steam curing

The efficiency of steam curing depends on various parameters such as delay period, the period of gradual increase in temperature, duration of maintaining constant maximum temperature, the period of the gradual decrease in temperature and cooling period.

Steam curing was done in steam curing chamber shown in Figure 3.5. A delay period (Pre-conditioning) of 4 hours, the rate of gradual increase in temperature $10^{\circ}\text{C}/\text{hour}$, curing period of 8 hours at a temperature of 60°C was adopted as steam curing scheme (Deogekar et al., 2013). After the cooling period (Post-conditioning) of 4 hours, specimens in the steam curing chamber were transferred to water curing tank where samples were immersed in water till testing age.

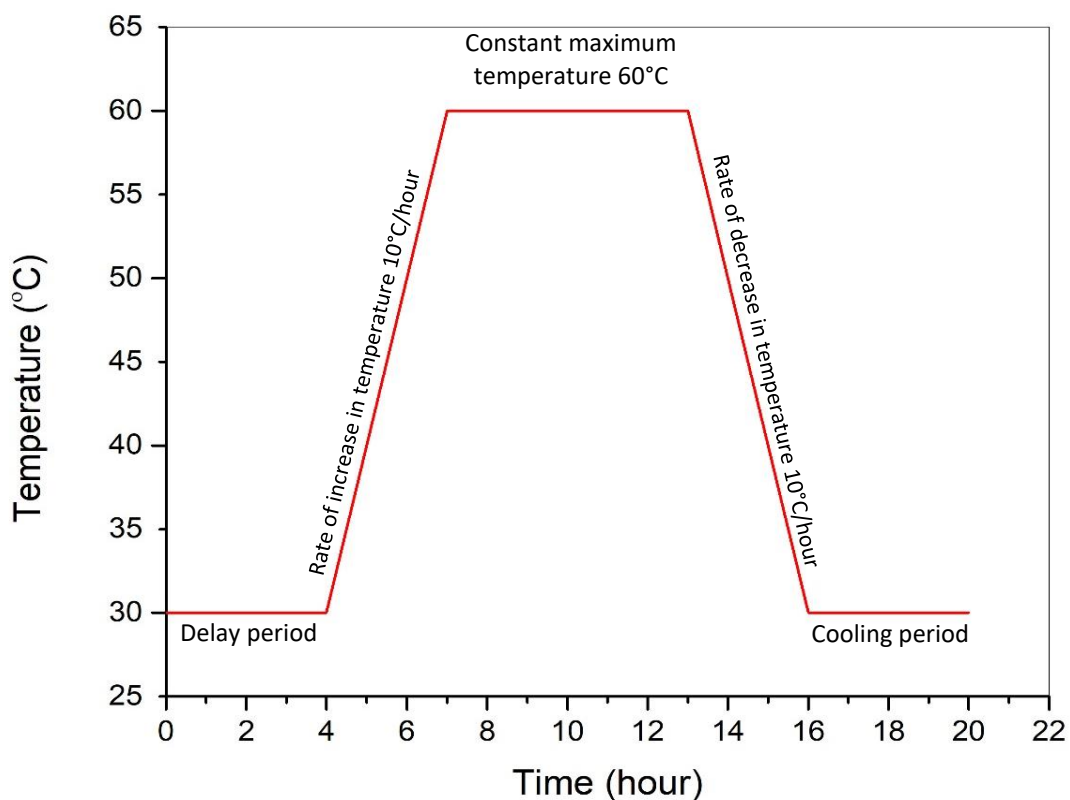


Figure 3.4: Steam curing scheme



Figure 3.5: Steam curing chamber

3.4.3 Accelerated carbonation curing

Figure 3.6 (a) and (b) show the basic carbonation curing set up and the carbonation chamber used in this study. An airtight vacuum chamber was used, and it was vacuumed before the injection of CO₂ gas. Pressure gauge and safety valve were installed with the CO₂ cylinder and the CO₂ gas used was 99% pure. The pressure at the time of injection was kept at 10 psi. Silica gel was kept at the bottom of the chamber to remove evaporated water from the specimens (*Baojian et al., 2013*). The specimens were kept inside the chamber for 6 or 12 hours for the curing purpose, and after that, they were placed in water for the subsequent water curing for 3 days. Once the 3 days water curing was finished, the samples were kept in the sealed plastic bags till the testing age.

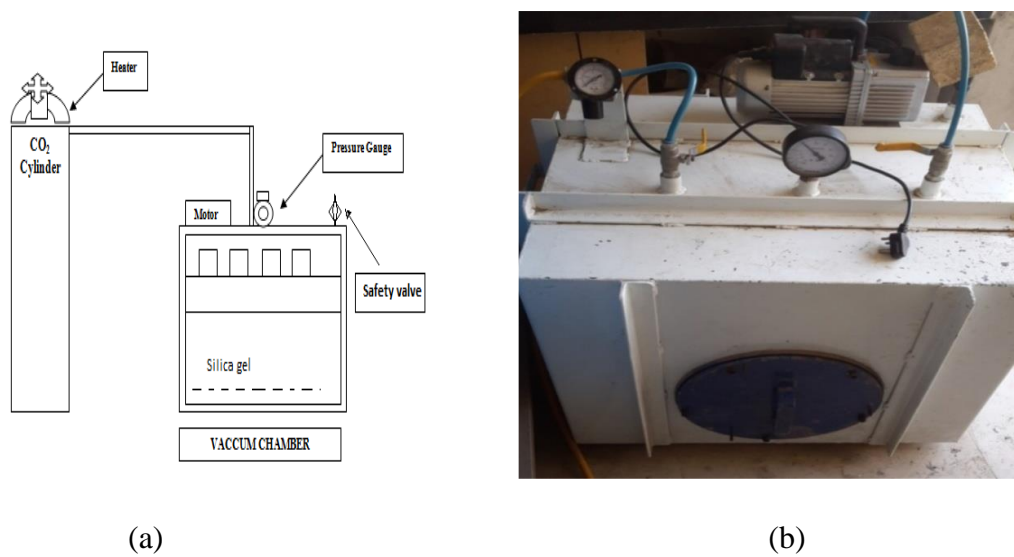


Figure 3.6: (a) Set up for carbonation curing chamber, and (b) Carbonation chamber used in this study

3.5 TESTING

This section describes in detail the tests conducted in this study and their experimental procedure. Tests were conducted on 3, 7 and 28-day of casting to examine compressive strength porosity and permeability of pervious concrete mix. Microstructure and morphology of pervious concrete were investigated at 3 and 28-day of casting using SEM, XRD and TGA analysis.

3.5.1 Compressive strength

The ability of a material or a structure to withstand a directly applied axial pushing force is termed as its compressive strength. Compressive strength is one of the most important and useful properties of pervious concrete. As a pavement material or in most of the other applications of pervious concrete, compressive stresses are the major stresses acting on pervious concrete.



Figure 3.7: Compression testing of cubes and tiles

For measurement of compressive strength of pervious concrete, cubes and interlocking tiles of dimensions given in Table 3.8 were cast. Compressive strength test was conducted at the age of 3, 7 and 28 days of casting. Compressive strength test was carried out on Automatic

Compression Testing Machine (ACTM). To remove the surface moisture, the specimens were surface dried after being taken out of the curing tank and kept outside at room temperature for half an hour. As per the procedure specified in BIS 516:1959 with loading rate of 140 kg/cm^2 , the cubes and interlocking tiles were placed in such a manner that the load was applied at a right angle to the face of the cube (BUREAU OF INDIAN STANDARDS, 2004). Figure 3.7 shows the testing of cube and interlocking tiles for compression under ACTM.

3.5.2 Porosity

Porosity is one of the main factors affecting the permeability of pervious concrete. The high porosity of pervious concrete was due to little to no fine aggregates content which provides percolation characteristics to pervious concrete. Porosity impacts permeability and compressive strength of pervious concrete and is dependent on mix proportions and method of compaction (*Rangelov et al., 2017*).

Porosity test was conducted in accordance with ASTM C 642 – 06 to measure the volume of permeable pore space (voids). Specimens of size $100 \times 100 \times 100 \text{ mm}$ were cast and tested at the age of 3, 7 and 28 days of casting. Porosity test was conducted in four steps as per procedure laid in ASTM C 642 06.

Step 1 - Oven dry mass: - Mass of specimens was determined at the age of 3, 7 and 28-days. To dry the specimens, specimens were placed in an oven at temperature 105 C for 48 hours. Mass of specimens was determined after specimens were removed from the oven and placed in dry air to reduce their temperature to 20 to 25 C . Difference between two successive values of mass of specimens was less than 0.5% of lesser value and hence accepted as per standard. Designate this oven-dry mass as A.

Step 2 – Saturated mass after immersion: - Specimens were immersed after step 1 in the water at 21 C temperature for 48 hours. Mass of surface dry specimens was measured after 48 hours and designate it as B-1. Specimens were immersed again for the next 24 hours and mass (B-2) of surface dry specimens was measured after 24 hours. Difference between B-1 and B-2 values of mass of specimens shown increase in mass of less than 0.5% of the B-2 value and hence accepted as per standard. Designate the final surface dry mass (B-2) as B.

Step 3 – Saturated mass after boiling: - Specimens were placed in the hot water bath chamber covered with tap water and boiled for 5 hours. Specimens after boiling were kept in air to allow

the natural loss of heat for 14 hours to lower temperature to 20 to 25 C. Then surface moisture of specimens was removed by towel and mass of specimens was determined and designated as C.

Step 4 – Immersed apparent mass: - Specimens after step 3 were suspended in water by wire in buoyant weight measuring equipment. Specimens submerged in water were vibrated for 10 minutes to remove any air present in voids of pervious concrete specimens. After vibration, the apparent mass of specimen was determined and designated as D.

Following equation as per ASTM C 642 – 06 was used for calculation of porosity.

$$\text{The volume of permeable space (voids), \%} = \frac{C-A}{C-D} \times 100 \quad \dots (3.1)$$

A = mass of oven-dry sample in the air (gm)

C = mass of surface dry sample in the air after immersion and boiling (gm)

D = apparent mass of sample in water after immersion and boiling (gm)

Average of three measurements was reported as a final result.

3.5.3 Permeability Test

In addition to compressive strength, the permeability of pervious concrete is another important property that indicates the performance of pervious concrete. There are number of factors on which permeability of pervious concrete depends like porosity, pore size distribution, pore roughness and connectivity of internal pore channels.

The permeability of the samples was tested at the ages of 3, 7 and 28 days of casting. In this method, a constant head permeability test was performed. Firstly specimen was saturated with water up to the brim, by passing the water through drainage pipe at *section-C* till water level rises and attains a constant level at *Section-B* and *C*. *Section-B* and *C* were at the same height from ground level. After achieving saturation, water was poured through the *section- A* with the help of pipe, and water level kept on rising till it attains the constant water head of 200 mm over a cylindrical specimen of 200mm in length and 100mm diameter. With the help of spill-out pipe and discharge of extra water through drainage pipe at *section-A*, the constant head was maintained at *section-A*. Once constant water head of 200mm was achieved, water collection

from drainage pipe at *section-C* was initiated for a period of 2 minutes (*Sandoval et al., 2017*). The lateral surface of cylindrical samples was tightly wrapped with impermeable membrane to prevent water leakage through sides Figure 3.9 (a) and (b), forcing the water entry only from the top surface and exit only from the bottom surface of the sample. The samples were placed inside a PVC pipe, and silicon gel was used to seal any gaps between the pipe and cylindrical samples. Figure 3.8 shows the permeability apparatus used for the present study. Following equation was adopted for calculation of permeability coefficient (*Sandoval et al., 2017*).

$$K = \frac{QL}{HA t} \quad \dots (3.2)$$

K = water permeability (cm/s)

Q = quantity of water collected (cm³)

L = specimen length (cm)

H = water head (cm)

A = cross sectional area of tested specimen (cm²)

t = time of water collection in seconds (s)

Average of three measurements was reported as a final result.

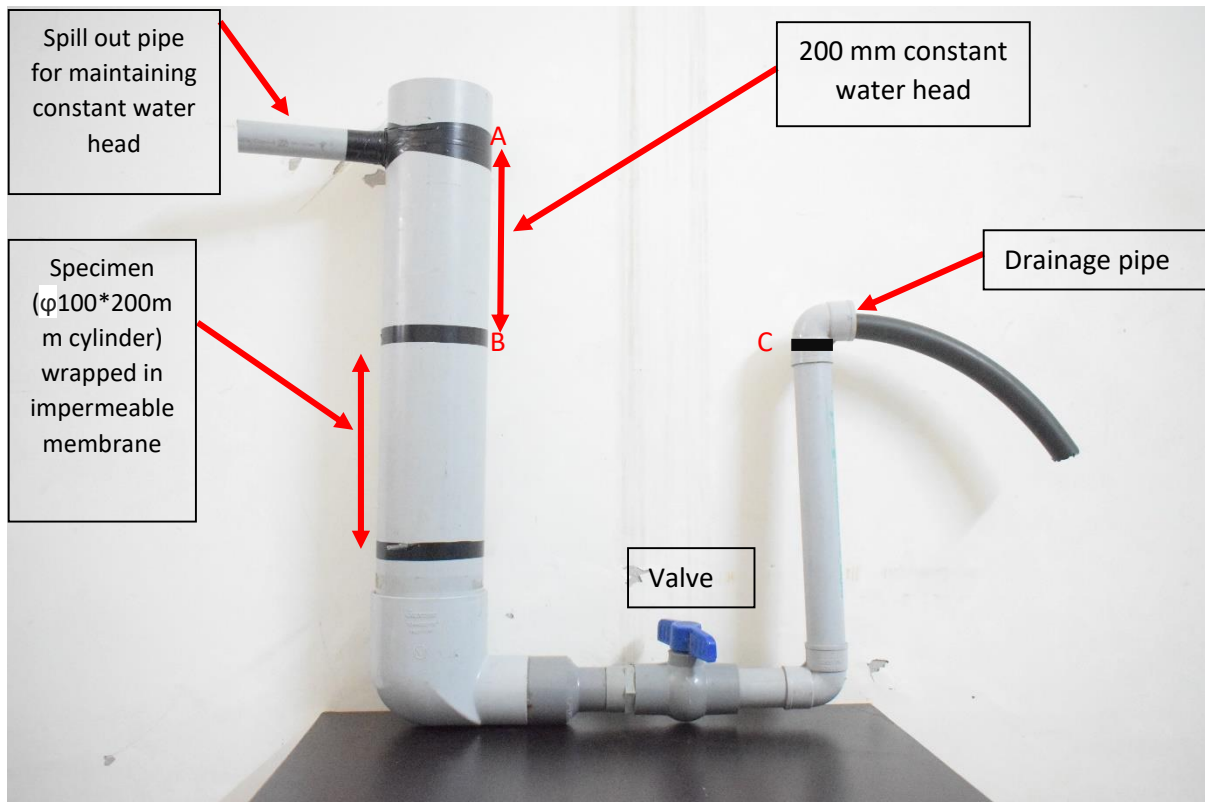


Figure 3.8: Water permeability test apparatus (*Sandoval et al., 2017*)



(a)



(b)

Figure 3.9 : (a) Specimen covered with PVC film (b) Specimen covered with conventional tape

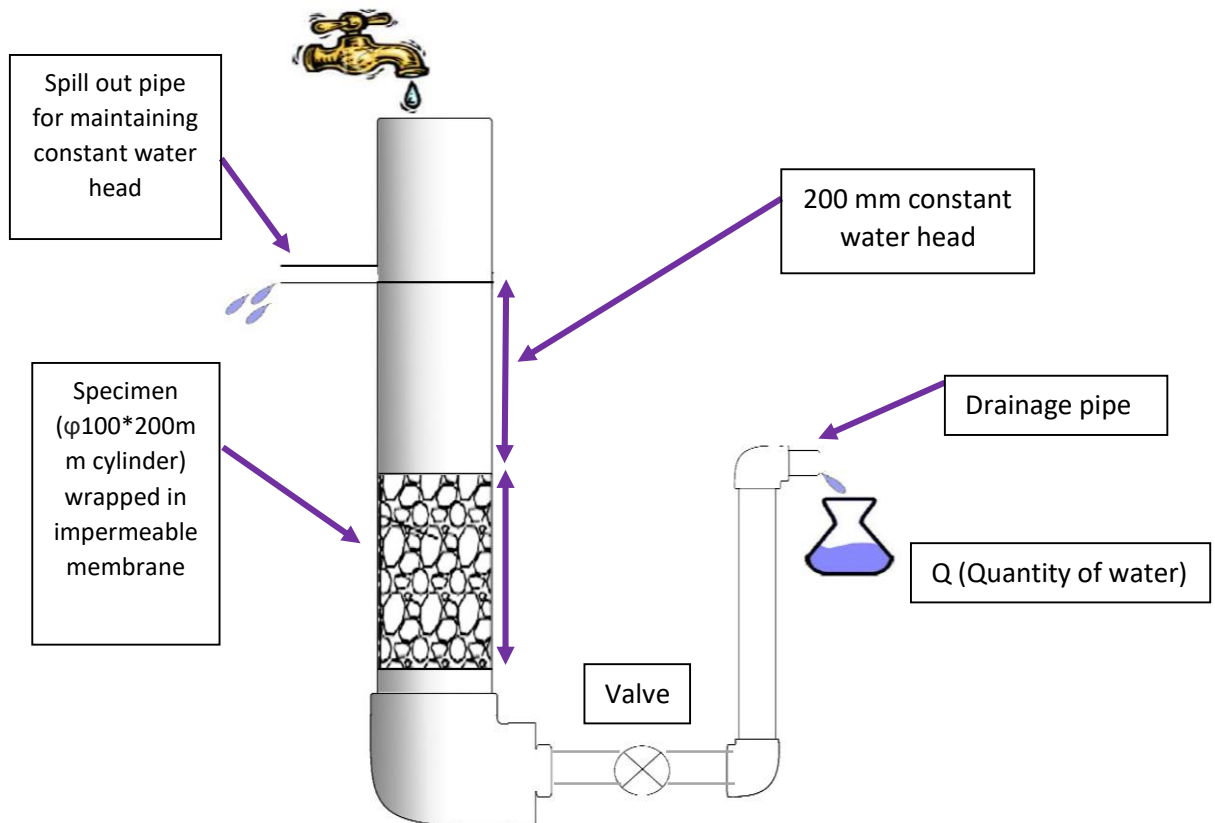


Figure 3.10: Schematic diagram of water permeability test apparatus

3.6 MICROSTRUCTURE ANALYSIS

Microstructure analysis of the concrete specimens was done through thermogravimetric analysis (TGA), X-ray diffraction studies (XRD), and scanning electron microscopy (SEM).

3.6.1 Thermogravimetric analysis (TGA)

The Thermogravimetric analysis was conducted to investigate the effects of ACC durations on CO₂ uptake, calcium carbonate and calcium hydroxide formation. TGA measures changes in mass in relation to changes in temperature. Mass loss curves provide information on the change in mass with an increase in temperature. The temperature range was kept from 0°C to 900°C and rate of increase of temperature was 10°C/min. The samples for TGA were taken from core of broken samples of compressive strength test. These samples were then grounded to fine powder and then finally passed through 80 µm sieve. The sample mass 10 g was used for TGA. The equations (3.3-3.5) were used for calculating percentage of CO₂ uptake, calcium carbonate and calcium hydroxide, respectively (*Chabannes et al., 2015; Zhang and Shao, 2016*). Calcium hydroxide calculated using equation 1.3 corresponding to mass loss from 400°C to 600°C which corresponds to dehydroxylation of calcium hydroxide. The amount of calcium carbonate was calculated from the loss of carbon dioxide (LCO₂) occurring between 600°C and 900°C.

$$\text{CO}_2 \text{ uptake (\%)} = \frac{\text{Sample mass at 550 }^\circ\text{C} - \text{Sample mass at 900 }^\circ\text{C}}{\text{cement mass in original sample}} \times 100 \quad \dots (3.3)$$

$$\text{CaCO}_3 \text{ (\%)} = \text{LCO}_2 \text{ (\%)} \times \frac{\text{Mw CaCO}_3}{\text{Mw CO}_2} \quad \dots (3.4)$$

$$\text{Ca(OH)}_2 \text{ (\%)} = \text{Mass loss between 400}^\circ\text{C and 600}^\circ\text{C} \times \frac{\text{Mw Ca(OH)}_2}{\text{Mw CO}_2} \quad \dots(3.5)$$

3.6.2 Scanning electron microscope (SEM) analysis

Scanning electron microscope (SEM) is a high magnification electron microscope which uses a focused beam of electrons to scan the sample and to produce highly magnified images of samples microstructure. SEM helps in identifying the morphology of mix; the morphology of the mix helps to analyze various physical and mechanical properties of the concrete mix. After the ages of 3 and 28 days of casting, the broken pervious concrete samples were taken after the compressive strength test for SEM analysis. For the removal of moisture before SEM analysis, the sample was placed in a desiccator for a period of 24h. The samples were gold coated and

placed on a brass stub using carbon tape. Then the microscopic image was obtained by scanning electron microscope (JOEL JSM 6510 LV, USA) at 15kV.



Figure 3.11: Scanning electron microscope (SEM).

3.6.3 XRD analysis

XRD analysis is a method for determination of the phases present in a particular material. X-ray powder diffraction technique is the most widely used technique to determine the structure of a material in bulk and thin-film forms. X'Pert PRO (PANalytical) diffractometer was used to obtain the XRD spectra with a Cu anode (40 kV and 30 mA) with a scanning angle of 10° to 70° . The samples were crushed, and ground and then they were mounted on a glass fibre filter with the help of a tubular aerosol suspension chamber (TASC). The components of the sample were determined by comparison with standards established by the International Center for Diffraction Data (ICDD). X-ray diffraction was based on the principle that the diffraction peaks are proportional to the substances producing them. The samples for the XRD analysis were taken from the inner part of the pervious concrete matrix after the compressive strength test. These samples were crushed and grounded to powder form and powder was finally passed through 300-micron sieve to obtain the fine powder, which was used as a sample for XRD analysis.

CHAPTER 4 - RESULTS AND DISCUSSION

4.1 GENERAL

In this chapter, results obtained from different tests conducted on pervious concrete subjected to different curing regimes at the age of 3, 7 and 28-days of casting are presented. The tests performed were compressive strength test, porosity and permeability tests. Further, in order to investigate the effect of different curing regimes on the microstructure of pervious concrete, SEM, XRD and TGA were conducted. The results and discussion based on the results obtained are presented in subsequent sections.

4.2 COMPRESSIVE STRENGTH

Pervious concrete specimens cured under different curing regimes at the ages of 3, 7 and 28-days of casting were tested for compressive strength. The test results are presented in Table 4.1 and Figure 4.1.

Table 4.1: Compressive strength test results at the ages of 3,7 and 28-days of casting

Curing scheme	Compressive strength (MPa)			% increase in compressive strength w.r.t water curing regime		
	3-days	7-days	28-days	3-days	7-days	28-days
WC	6.32	8.22	10.54	-	-	-
SC	9.45	10.29	12.47	+49.5 %	+25.1 %	+18.3 %
C-6	6.89	7.96	9.70	+9.1 %	-3.1 %	-7.9 %
C-12	9.05	11.93	15.20	+43.2 %	+45.1 %	+44.1 %

Figure 4.1 shows that the 3-day compressive strength was highest for steam cured specimens followed by accelerated carbonation curing (ACC) specimens. The lowest compressive strength was attained by water cured specimens. At the age of 7-days and 28-days, the highest value of compressive strength was attained by C-12 specimens followed by steam cured specimens.

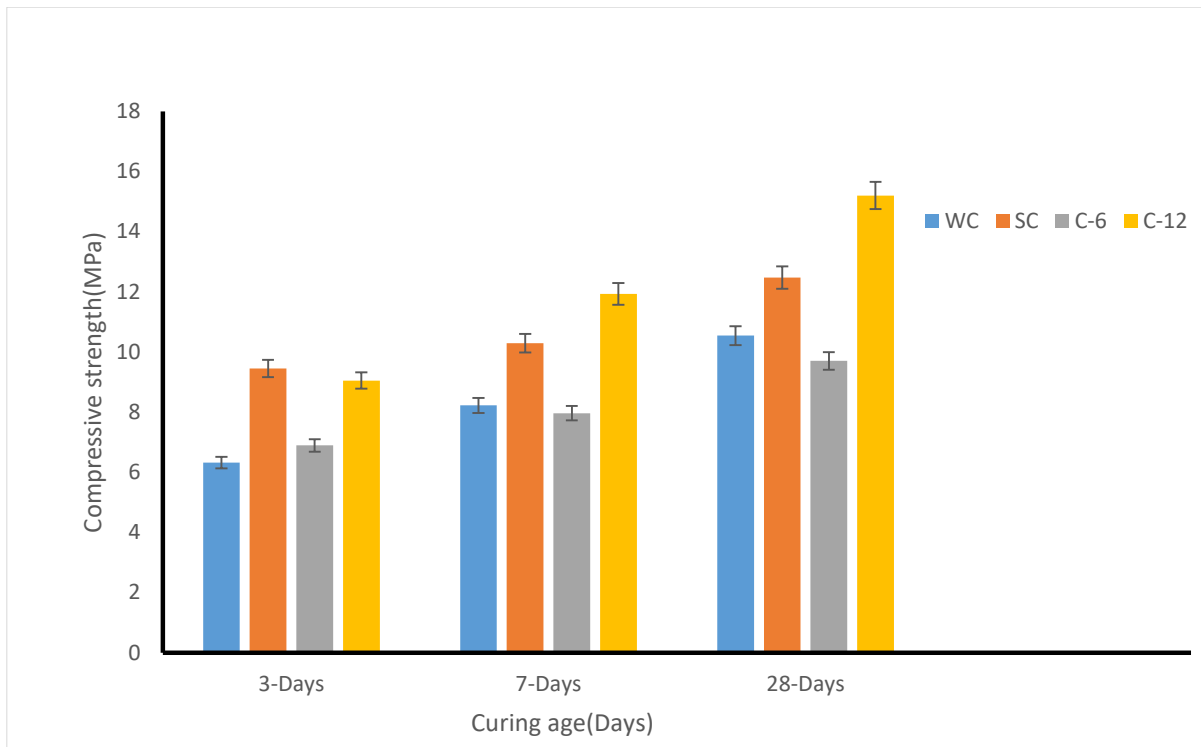


Figure 4.1: Compressive strength test results at the ages of 3, 7 and 28-days of casting

The compressive strength attained by all the curing regimes was higher than the minimum required compressive strength of 10 MPa for drainage pavement, precast concrete products and stone protection (Rafique et al., 2012).

Steam curing and carbonation curing regimes attained higher compressive strength than the traditionally used water curing technique. Steam cured specimens attained 49.5 % higher 3-day compressive strength as compared to WC. This strength gain can be attributed to the fact that the rate of hydration of cement increases with increase in temperature. As a result of which rapid formation of hydration product C-S-H gel takes place that improves the microstructure and increases the density of SC treated specimens. Similar results for compressive strength of SC specimens has been reported in earlier researches (Deogekar et al., 2013). Subsequent water curing of SC samples after cooling period till testing age, provides the water required for hydration to continue, which further forms additional C-S-H gel and increases compressive strength. Steam curing specimens were able to achieve a sufficient degree of hydration and hence, higher density and strength gel as compared to WC.

C-12 specimens attained 45.1 and 15.9% at 7-day, 44.1 and 21.8% at 28-day higher compressive strength than WC and SC counterparts respectively. CO₂ passed into pervious

concrete through ACC reacts with compounds of calcium present in concrete and leads to the formation of stable CaCO_3 from $\text{Ca}(\text{OH})_2$, and calcium-silicate-hydrocarbonate gel from unhydrated cement components. Calcium carbonate has a higher density and hardness as compared to calcium hydroxide due to which the microstructure densifies (Neves et al., 2015). As the rate of carbonation reaction was higher than the rate of hydration reaction, due to which rapid as well as more formation of carbonation reaction products and accelerated strength gain takes place. Calcium-silicate-hydrocarbonate gel possesses better gel structure than C-S-H gel provided by WC (Rostami et al., 2012). ACC was followed by 3-day WC; this provides water for further hydration of uncarbonated cement at later age and further increases the compressive strength of C-12 specimens (He et al., 2016; Sharma and Goyal, 2018). The higher amount of formation of carbonation reaction products during ACC, results in an increase in density and denser microstructure and provides better mechanical and durability properties (Mo et al., 2017; Panesar and Mo, 2013; Rostami et al., 2012).

C-6 specimens had higher 3-day compressive strength as compared to WC specimens. This higher strength can be attributed to the reactions involved in the carbonation process. In the case of C-6, reaction with carbon dioxide causes conversion of calcium hydroxide to calcium carbonate. The rate of carbonation reaction was higher than the rate of hydration reaction (He et al., 2017) due to which rapid as well as more formation of carbonation reaction products C-S-H gel and CaCO_3 , and hence, accelerated strength gain takes place. As ACC is an exothermic reaction, it leads to loss of water from cement paste, which decreases the amount of remaining water content required to carry out the hydration reaction. To compensate for this loss of water, ACC was followed by 3-day WC. This post carbonation water curing provides moisture for hydration reaction to continue (He et al., 2016). Further continuation of hydration reaction results in the formation of additional C-S-H gel and further increases in compressive strength. A higher amount of formation of C-S-H gel in C-6 specimens as compared to WC counterparts and precipitation of CaCO_3 increases density and improves the microstructure of C-6 specimens that leads to higher 3-day compressive strength.

There is no significant increase in the value of compressive strength of C-6 specimens at the testing age of 7 and 28-day of the casting was observed. It can be concluded from this observation that 3-day WC after 6 hours of ACC does not provide enough moisture for hydration reactions to take place as compared to WC specimens up to 7 and 28-day of casting.

As a result of this, no significant improvement in compressive strength was observed in C-6 specimens as compared to WC specimens.

C-12 specimens were able to achieve higher compressive strength than the C-6 specimens. The higher duration of carbonation in C-12 specimens tend to sequester more CO₂ in concrete. The greater content of CO₂ results in more CaCO₃ and calcium-silicate-hydrocarbonate in C-12 than C-6 (Ahmad et al., 2017; Huntzinger et al., 2009; Neves et al., 2015). This results in higher compressive strength and denser microstructure in C-12 specimens.

4.2.1 Strength development rate

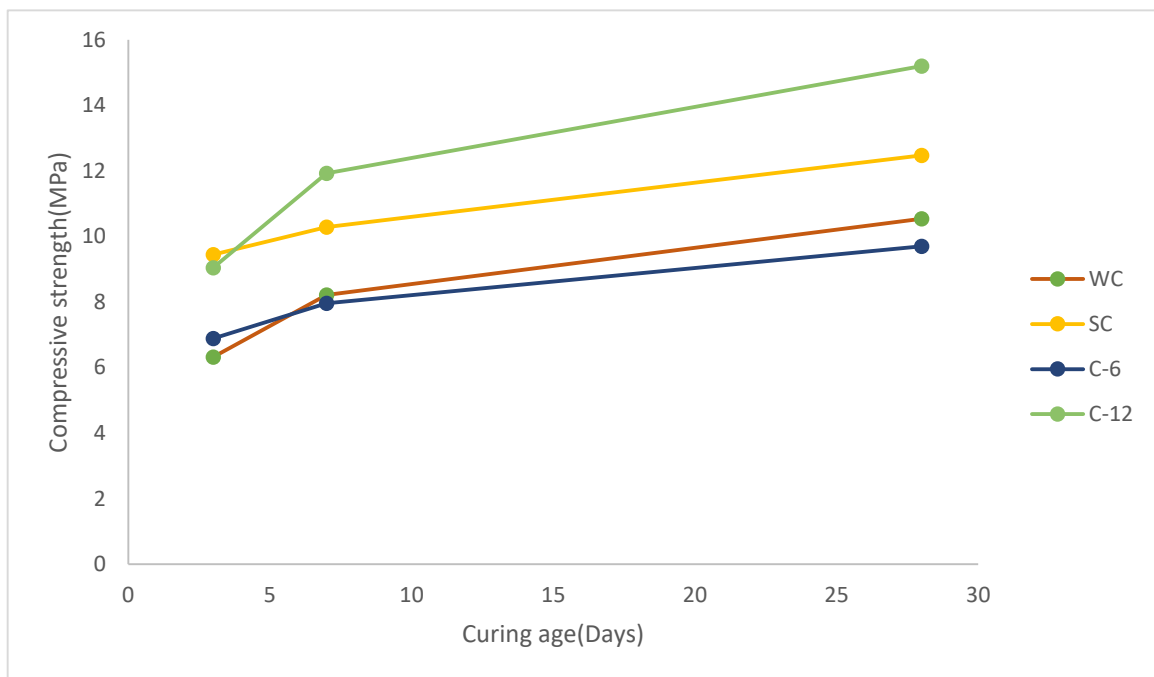


Figure 4.2: Compressive strength development rate of different curing regimes

Effects of different curing regimes on compressive strength development rate are presented in Figure 4.2. Rate of strength development was significantly higher for C-12 in the time period of 3 to 7 days as compared to other curing regimes. This greater strength gain can be attributed to the formation of CaCO₃ that acts as a nucleation site for further hydration reactions. This results in a higher rate of hydration and hence, higher compressive strength gain. The rate of strength gain post 7 days was similar for all the curing regimes.

4.3 POROSITY

Porosity test of pervious concrete specimens cured under different curing regimes was conducted at the ages of 3, 7 and 28-days of casting and the results are presented in Table 4.2 and Figure 4.3.

Table 4.2: Porosity test results at the ages of 3, 7 and 28-days of casting

Curing scheme	Porosity(%)			% increase in porosity w.r.t water curing regime		
	3-day	7-day	28-day	3-day	7-day	28-day
WC	23.77	22.43	20.97	-	-	-
SC	26.82	23.03	20.17	+12.83%	+2.67%	-3.81%
C-6	20.98	19.56	18.68	-11.74%	-12.79%	-10.92%
C-12	17.26	15.76	14.10	-27.39%	-29.74%	-32.76%

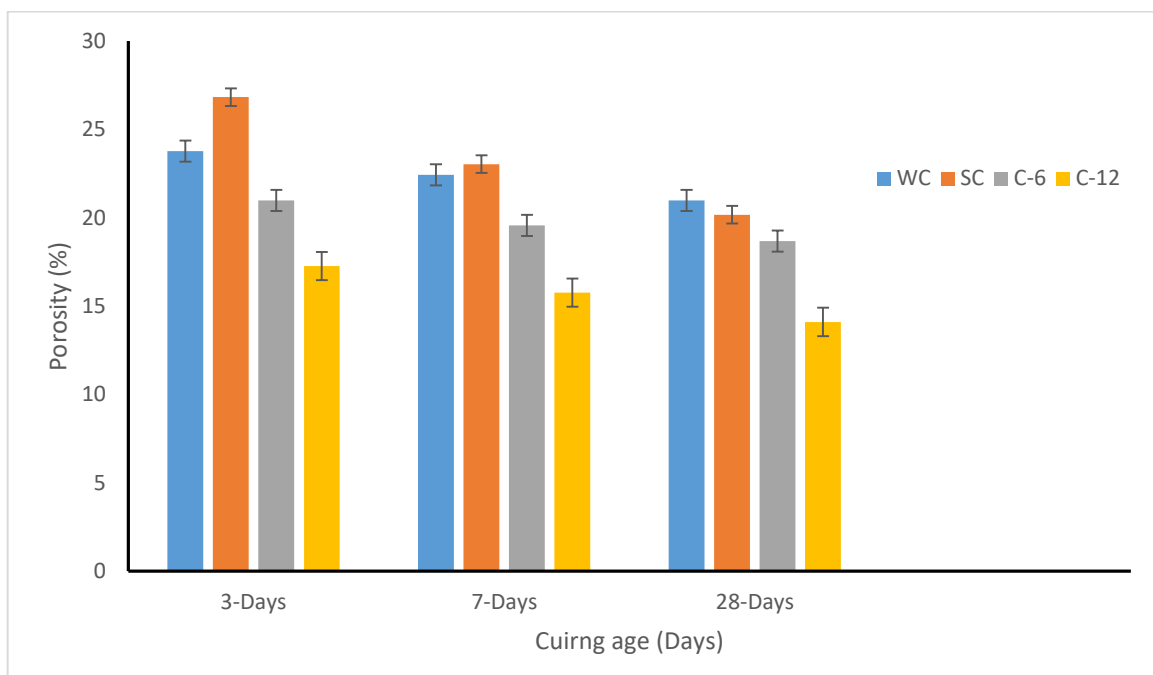


Figure 4.3: Porosity test results at the ages of 3, 7 and 28-days of casting

Figure 4.3 shows that the lowest porosity was achieved by ACC cured specimens at all testing ages. Among the two types of carbonation curing regimes(C-6 and C-12), C-12 achieved the least porosity followed by C-6. This trend was similar at all the curing ages. SC specimen

achieved the highest porosity followed by WC specimen for 3 and 7-day porosity testing, while 28-day porosity was highest for WC specimen followed by SC counterparts. It was observed that porosity varied from 14.1 to 26.82 % irrespective of curing regimes, which is acceptable as recommended porosity ranges from 15 to 25 % (*Rafique et al., 2012*).

ACC cured specimens achieved the lowest porosity as compared to steam and water cured counterparts. C-12 had 32.76, 30.09, and 24.52 % lower 28-day porosity as compared to WC, SC and C-6 specimens respectively. Carbonation reaction led to the conversion of unhydrated compounds of calcium in cement and hydration product Ca(OH)_2 into CaCO_3 . Carbonation of C_3S , C_2S , CH and C-S-H causes an increase in solid volume by 92.5, 108.7, 11.5, and 23.1% respectively as reported (*Ahmad, 2018*). Increase in the amount solid phase due to precipitation of CaCO_3 in the pore network of ACC specimens leads to decrease in pore connectivity and reduced porosity (*Rostami et al., 2011*). Subsequent water curing for 3-days following ACC bring about the hydration of unreacted cement particles and provide additional CSH gel and denser microstructure which further reduces porosity. The fine particles of CaCO_3 precipitated particles provide nucleation points for the hydration of tri-calcium silicate, which generates accelerated hydration of tri-calcium silicate. This causes micro-aggregation effect, which results in denser microstructure and causes significant reduction in porosity (*Qian et al., 2016*).

C-12 specimens were able to achieve lower porosity than the C-6 specimens. The higher duration of carbonation in C-12 specimens tend to sequester more CO_2 in concrete. The greater content of CO_2 results in more CaCO_3 and calcium-silicate-hydrocarbonate in C-12 than C-6 (*Ahmad et al., 2017; Huntzinger et al., 2009; Neves et al., 2015*). This results in a denser microstructure and lower porosity in C-12 as compared to C-6 specimens.

C-6 specimens were less porous than WC and SC specimens, whereas the compressive strength of the C-6 specimens was lesser than the other curing regimes. This can be attributed to the fact that ACC has a more dominating effect on surface as compared to the core. Therefore, in case of C-6 specimens the carbonation reactions took place at near-surface of concrete, whereas in case of C-12 CO_2 was able to penetrate to a greater depth and carbonate the paste at the core also. This resulted in a higher compressive strength for C-12 specimens, but not for C-6 specimens.

Significant porosity difference of C-12 specimen and all other curing regimes can be attributed to sufficient carbonation due to the higher duration of ACC, that causes more CO₂ to be sequestered into concrete and also, availability of enough moisture due to 3-day WC following ACC which results in the continuation of hydration reaction of C-12 specimen. This indicates a higher content of carbonation and hydration products in C-12 specimens, which results in denser microstructure and reduced porosity (*Qian et al., 2016*). Water cured specimens also had higher 28-day compressive strength and porosity as compared to C-6 specimens. Similar trends between porosity and compressive strength have been reported by earlier researchers (*Sharma and Goyal, 2018*).

On the other hand, Steam cured specimen had 35.65, 21.77 and 12.83 % higher 3-day porosity compared to C-12, C-6 and WC regime specimens respectively. This higher porosity can be attributed to the fact that elevated temperature during SC treatment causes faster hydration and heterogeneous distribution of hydration products, which causes the formation of large pores in the hardened paste and higher porosity (*Qian et al., 2016; Zhi-min et al., 2012*). Elevated temperature damages the concrete surface directly exposed to it by introducing micro-cracks and coarsening the pore structure of the exposed surface (*Zou et al., 2018*). However, the adverse effects of steam curing regime can be eliminated by introducing water curing as subsequent curing following initial steam curing, leading to refinement of pore structure of concrete and reduces inhomogeneity in SC treated specimens. The difference of porosity between WC and SC specimens at the age 7-days and 28-days was lesser as compared to 3-day porosity. This can be explained based on the formation of hydration products on subsequent WC and their distribution, which led to more homogenous and denser microstructure. A decrease in median pore diameter of steam-cured concrete to a value lower than water cured specimens at 28 days has been reported by earlier researchers (*Zhi-min et al., 2012*).

4.3.1 Relationship between compressive strength and porosity.

Compressive strength for all curing regimes showed an increase with the decrease in porosity, with curing age as shown in Figure 4.4. The highest and lowest rate of increase in compressive strength with a decrease in porosity was observed for C-12 and SC specimens, respectively. Which was in agreement with compressive strength test results.

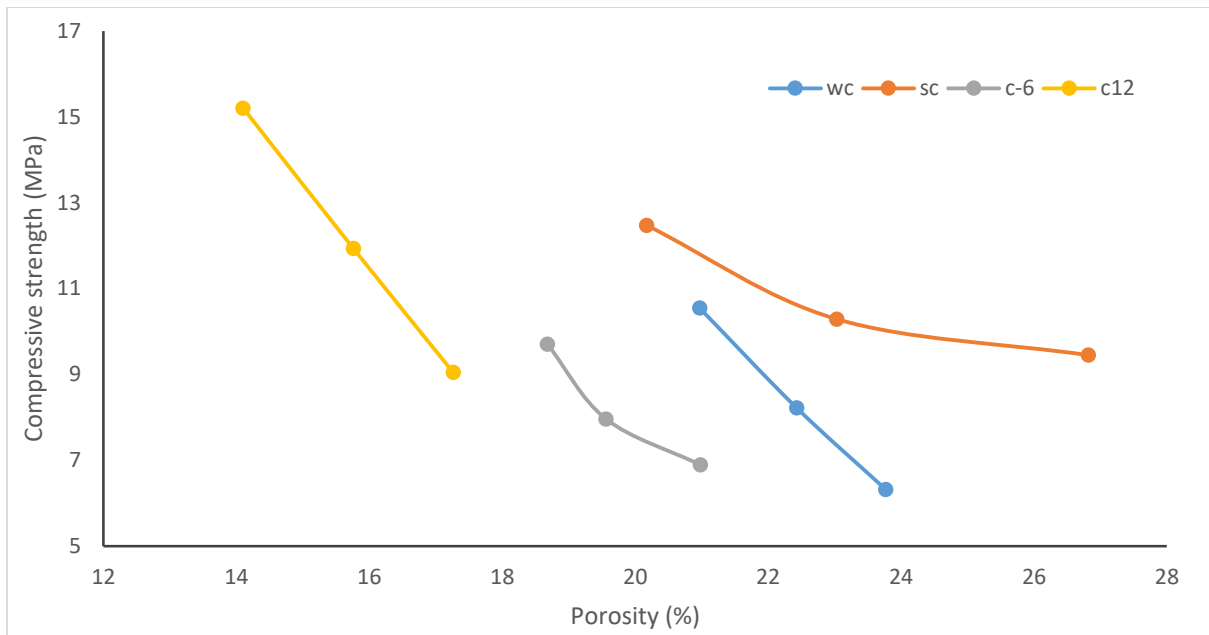


Figure 4.4: Relationship between compressive strength and porosity

4.4 PERMEABILITY

The results of the permeability test of pervious concrete specimens cured under different curing regimes at the ages of 3, 7 and 28-days of casting are presented in Table 4.3 and Figure 4.5.

Table 4.3: Permeability test results at the ages of 3, 7 and 28-days of casting

Curing scheme	Permeability(cm/s)			% increase in permeability w.r.t water curing regime		
	3-day	7-day	28-day	3-day	7-day	28-day
WC	2.88	2.69	2.46	-	-	-
SC	3.64	2.95	2.27	+26.39%	+9.67%	-7.72%
C-6	2.29	2.07	1.87	-20.49%	-23.05%	-23.98%
C-12	1.68	1.42	1.28	-41.67%	-47.21%	-47.97%

Figure 4.5 shows that the lowest permeability was achieved by ACC cured specimens at 3, 7 and 28-day of casting. C-12 had lowest 3, 7 and 28-day permeability was also in agreement with its porosity results. SC specimen achieved the highest permeability followed by WC for 3 and 7 day permeability testing, while 28-day permeability was highest for WC specimen followed by SC counterparts.

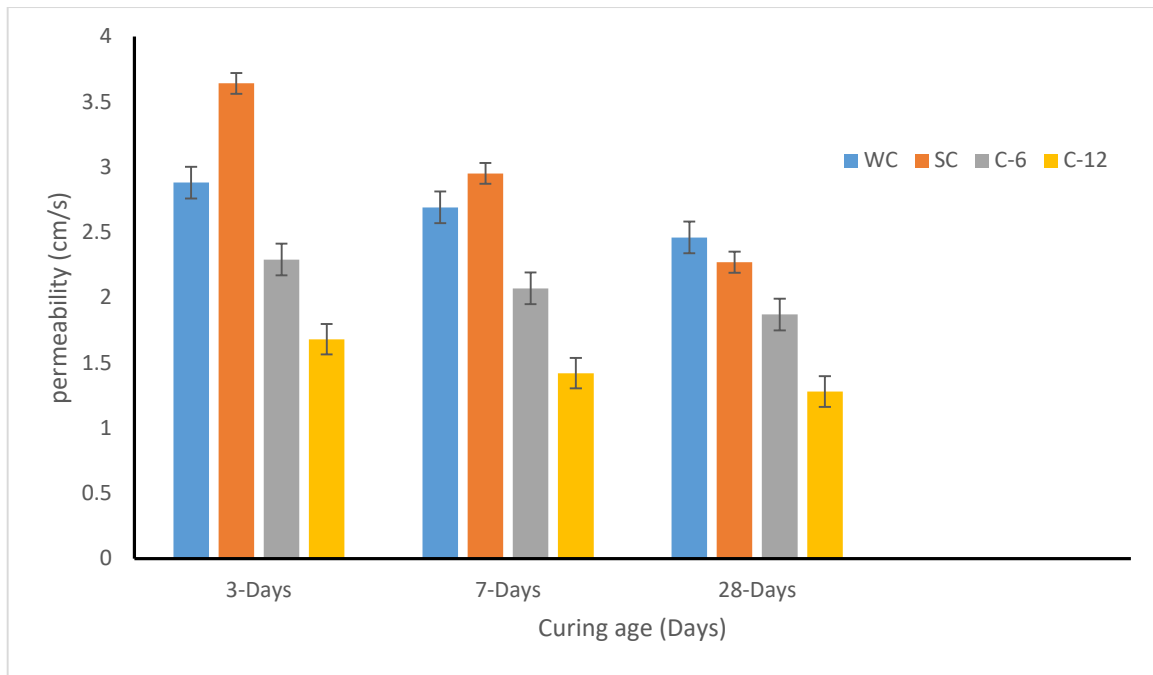


Figure 4.5: Permeability test results at the ages of 3,7 and 28-days of casting

It was observed that permeability coefficient value varied from 1.28 to 3.64 cm/s irrespective of curing regimes, which is acceptable as recommended permeability coefficient value ranges from 0.25 to 3.3 cm/s (*Rafique et al., 2012*). Lowest permeability was achieved by ACC cured specimens at 3, 7 and 28-day of casting which was in agreement with porosity results.

CO₂ sequestered into pervious concrete during ACC reacts with cement compounds such as calcium silicates, AFt, AFm and hydration products CH and C-S-H. Products of these carbonation reactions such as calcium carbonate increased the amount of solid volume (*Ahmad, 2018*) and led to micro-aggregate effect due to precipitated CaCO₃ (*Qian et al., 2016*). This causes a significant decrease in pore connectivity and increases pore tortuosity. Permeability was inversely related to tortuosity as reported by earlier researchers (*Ahmed et al., 2005*). Subsequent water curing for 3-days following acc leads to hydration of unreacted cement paste and provide additional CSH gel and denser microstructure, which further reduces pore connectivity. Lowest permeability of C-12 specimen can be attributed to sufficient carbonation and hydration, which led to a higher amount of carbonation and hydration products, respectively (*Qian et al., 2016*).

Steam cured concrete had the highest 3 and 7-day permeability compared to other regime specimens. This was because the elevated temperature during SC treatment results in a

heterogeneous distribution of hydration products, micro-cracks and coarsening the pore structure which increases pore-connectivity and reduces tortuosity, thereby increasing permeability (*Qian et al., 2016; Zhi-min et al., 2012*). 28-day permeability of steam cured specimen was lower as compared to water cured specimen. This was due to subsequent water curing SC specimens which helped in achieving denser pore structure by ensuring sufficient moisture for continuation hydration reaction and hence providing additional CSH gel and more homogenous distribution of hydration products (*Zhi-min et al., 2012*). Generally, Compressive strength of concrete increases with a decrease in porosity, and permeability increases with an increase in porosity. However, due to certain factors, such as micro-aggregate effect in pores, pore size distribution, pore roughness, pore connectivity, and pore tortuosity, these relations might not hold always as reported by various previous studies (*Barišić et al., 2017; Ramkrishnan et al., 2018; Sharma and Goyal, 2018*).

4.5 EFFECT DURATION OF ACC ON CARBONATION PRODUCTS AND CO₂ UPTAKE

Results of TGA are shown in Figure 4.6 and Table 4.4. Mass loss curves in Figure 4.6 from TGA analysis of ACC cured specimens at the age of 28-days of casting showed the higher formation of calcium hydroxide and calcium carbonate for C-12 as compared to C-6 specimen. The CO₂ uptake calculated from thermogravimetric analysis mass loss curve using equation (3.3) was 6.82 and 4.75 % for C-12 and C-6, respectively. Which indicate 43.5% higher CO₂ uptake for C-12 specimen as compared to the C-6 specimen. This indicates that more CO₂ was absorbed in C-12 as compared to C-6, due to higher duration (12 hours) of curing. This confirms enhanced carbonation and hydration of C-12 specimen as compared to C-6 specimen, which is in agreement with compressive strength, porosity, and permeability tests results.

Table 4.4: Percentage of compounds present in ACC cured specimens

S.NO	Compound	Percentage (%)	
		C-12	C-6
1	Calcium carbonate	14	9.6
2	Calcium hydroxide	4.0	2.4

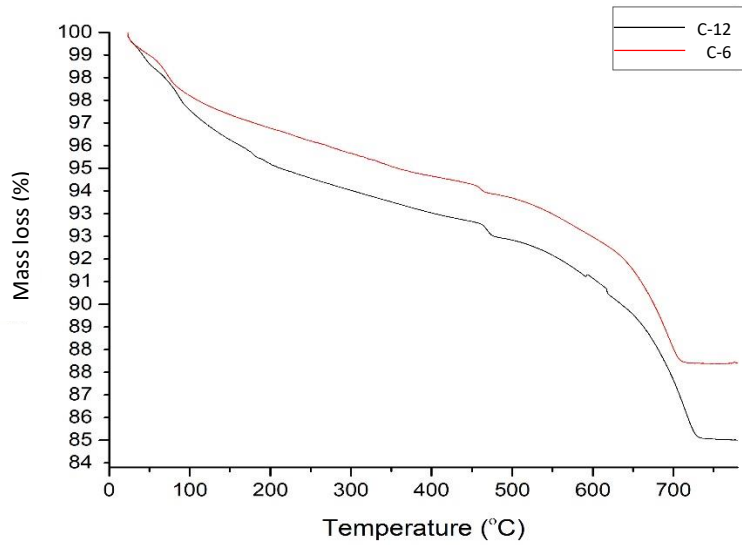


Figure 4.6: Mass loss curve of ACC cured specimens

4.6 XRD ANALYSIS

XRD analysis was performed for determination of the phases present in the cement paste of pervious concrete subjected to different curing regimes. Figure 4.7 and 4.8 shows XRD analysis results at the age of 3 and 28-days of casting, respectively.

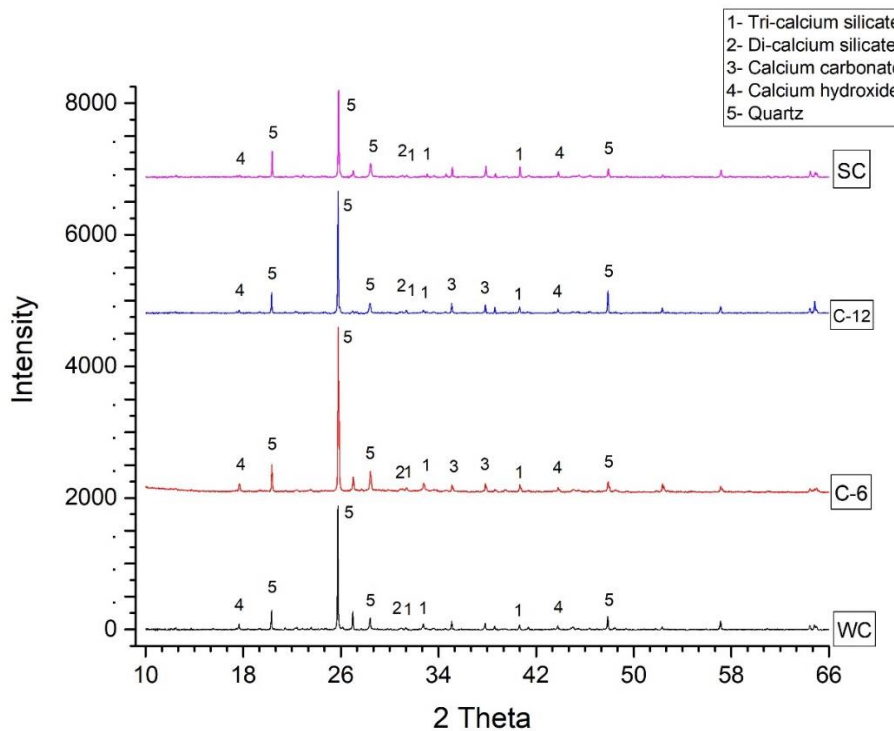


Figure 4.7: XRD analysis of different curing regimes after 3 days of casting

XRD analysis of WC regime shows strong peaks of calcium hydroxide (CH), quartz, tricalcium silicate(C₃S) and dicalcium silicate(C₂S). The intensity of CH Peaks was lesser for WC as compared to SC due to the higher rate of hydration in SC, and subsequent water curing in SC regime aids hydration of cement.

Three day XRD analysis shows strong peaks of quartz and CH in SC specimen as compared to other curing regimes. This confirms greater CSH formation, which provides higher strength as observed in 3-day compressive strength results. C-12 specimen showed diminished peaks of CH due to the conversion of CH to CaCO₃ by CO₂ during carbonation. Strong peaks of CaCO₃ confirms sufficient carbonation of C-12 specimen. Peaks of CH in C-12 confirms, further hydration on subsequent water curing following ACC.

The intensity of CaCO₃ peaks was lesser in C-6 specimen as compared to C-12 as shown in Figure 4.7. CH peak was stronger for C-6, which was due to insufficient carbonation of C-6 specimen, due to which all of Ca(OH)₂ produced during initial hydration was not converted to CaCO₃. This further confirms that 6 hours duration of ACC was not enough for sufficient carbonation of cement paste.

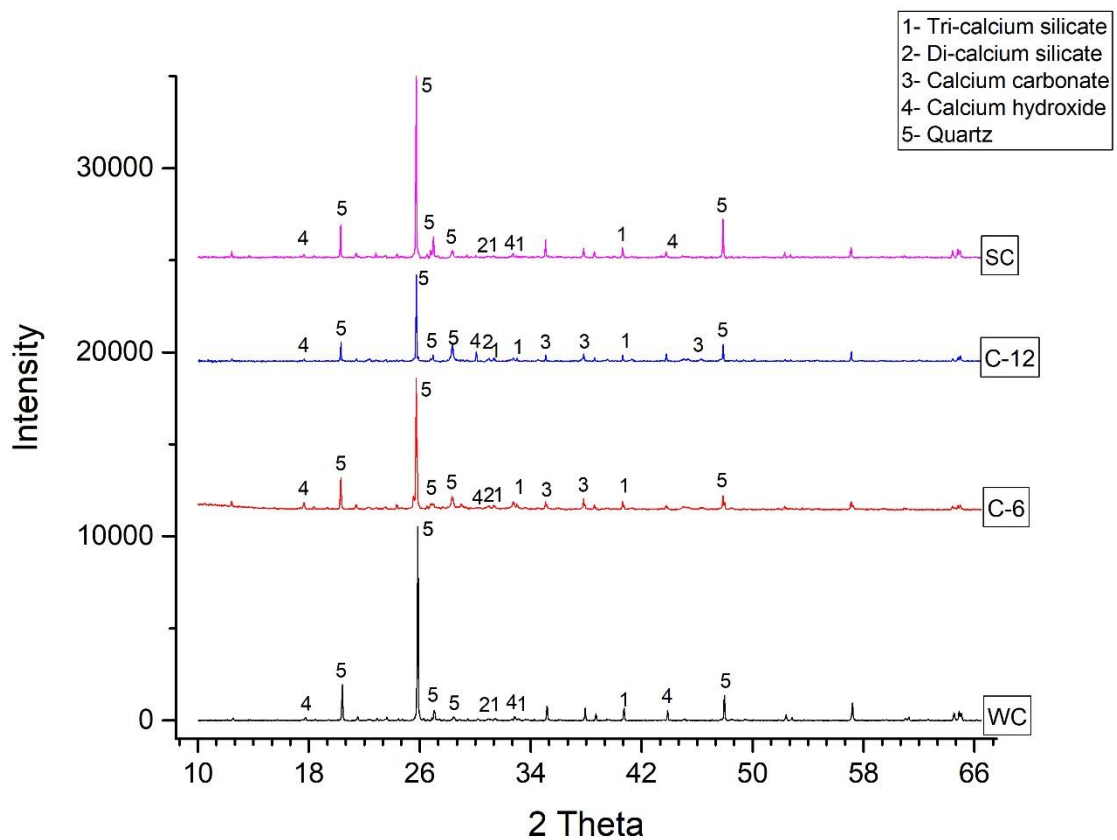


Figure 4.8: XRD analysis of different curing regimes after 28 days of casting

Figure 4.8 gives the XRD analysis for different curing regimes at the age of 28 days. XRD analysis of C-12 specimen shows strong peaks of CaCO_3 and CH, which confirms sufficient carbonation through ACC and enough hydration through subsequent 3 days of water curing post carbonation. This was evidence for greater formation of carbonation and hydration products in C-12 as compared to other regime counterparts and was in agreement with the highest 28-day compressive strength of C-12 specimen. Strong peaks of CH confirmed sufficient hydration reaction in C-12 specimen post carbonation. In the case of C-6 specimen, lower intensity of CH and CaCO_3 peaks was observed, indicating inadequate carbonation and hydration of specimen in C-6 regime. SC specimen shows strong peaks of CH and silica gel as compared to WC counterpart, which confirms sufficient CSH gel formation owing to subsequent water curing following SC till testing the age of 28 days of casting.

4.7 SEM ANALYSIS

The four curing regimes were further examined at the microscopic level to understand morphology of resultant pervious concrete subjected to different curing regimes. Figure 4.9 and 4.10 shows images of SEM analysis conducted on pieces of broken specimens of compressive strength test at the age of 3-day and 28-day of casting, respectively.

It can be seen in SEM images of Figure 4.9, CSH gel formation was greater for SC, followed by ACC and least in case of WC specimen at the age of 3 days of casting.

SC specimen image Figure 4.9(b) at the age of 3 days shows higher formation of CSH as compared to water curing regime. This was due to a higher rate of hydration during initial SC which provides greater amount of CSH gel, and subsequent water curing following SC till the age of testing provides additional CSH gel. This was also in agreement with compressive strength results at the age of 3-days of casting.

With the presence of CaCO_3 due to ACC along with CSH, as seen in Figure 4.9(d), C-12 shows denser microstructure. Presence of CH confirms further hydration of C-12 specimen on subsequent water curing after ACC.

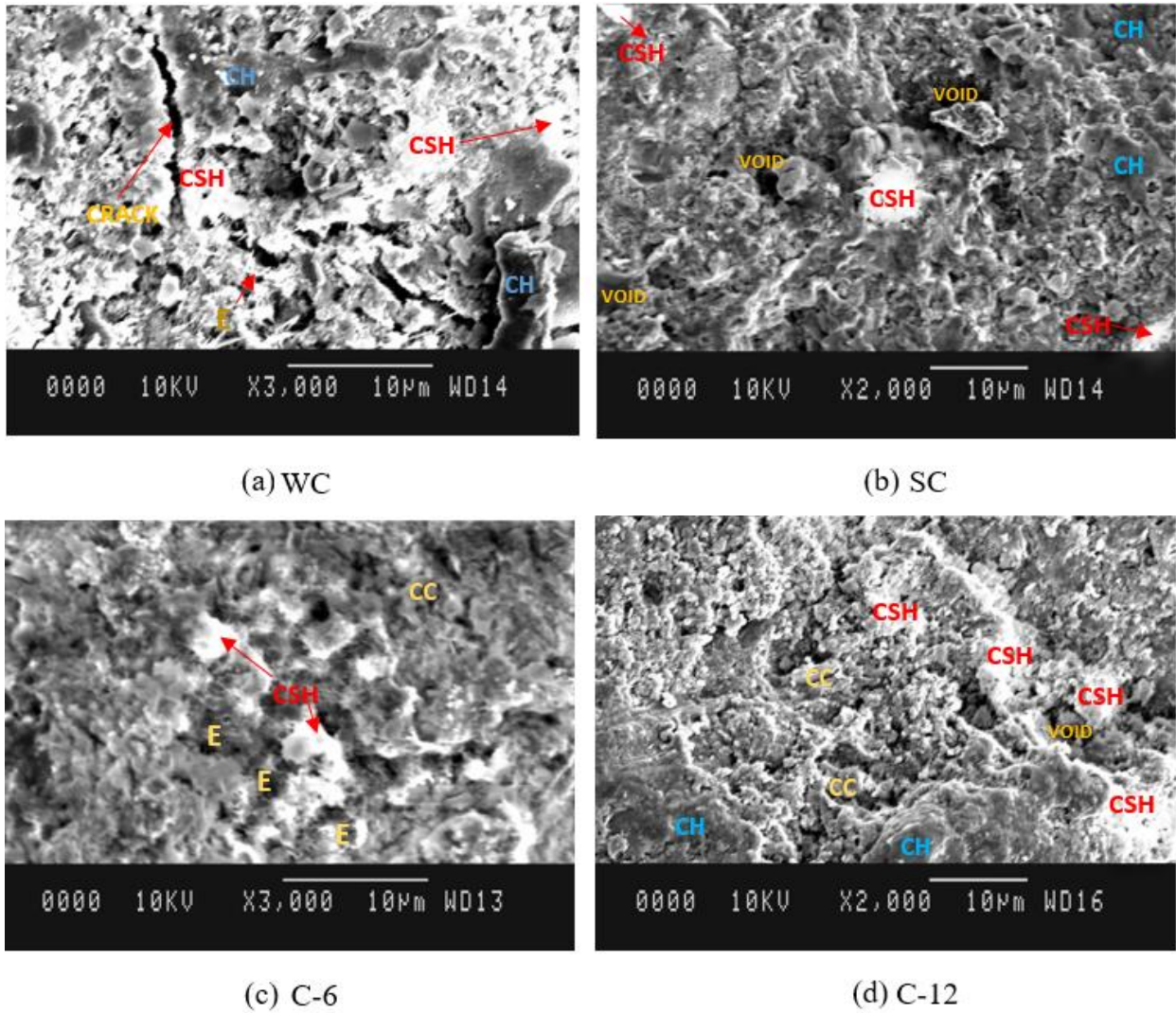


Figure 4.9: SEM analysis of four different curing regimes at the age of 3-days of casting

As shown Figure 4.9(c), C-6 has a comparatively less dense microstructure and CaCO_3 presence, and higher $\text{Ca}(\text{OH})_2$ as compared to C-12 specimen. This indicates lesser carbonation in case of C-6 specimen. Due to lesser carbonation, there was a reduced presence of CaCO_3 and higher $\text{Ca}(\text{OH})_2$ in C-6 specimen. Presence of CaCO_3 produces micro aggregate effect and clogging of pores, this results in a decline in porosity, which was confirmed in porosity test results with C-6 and C-12 having the lowest porosity.

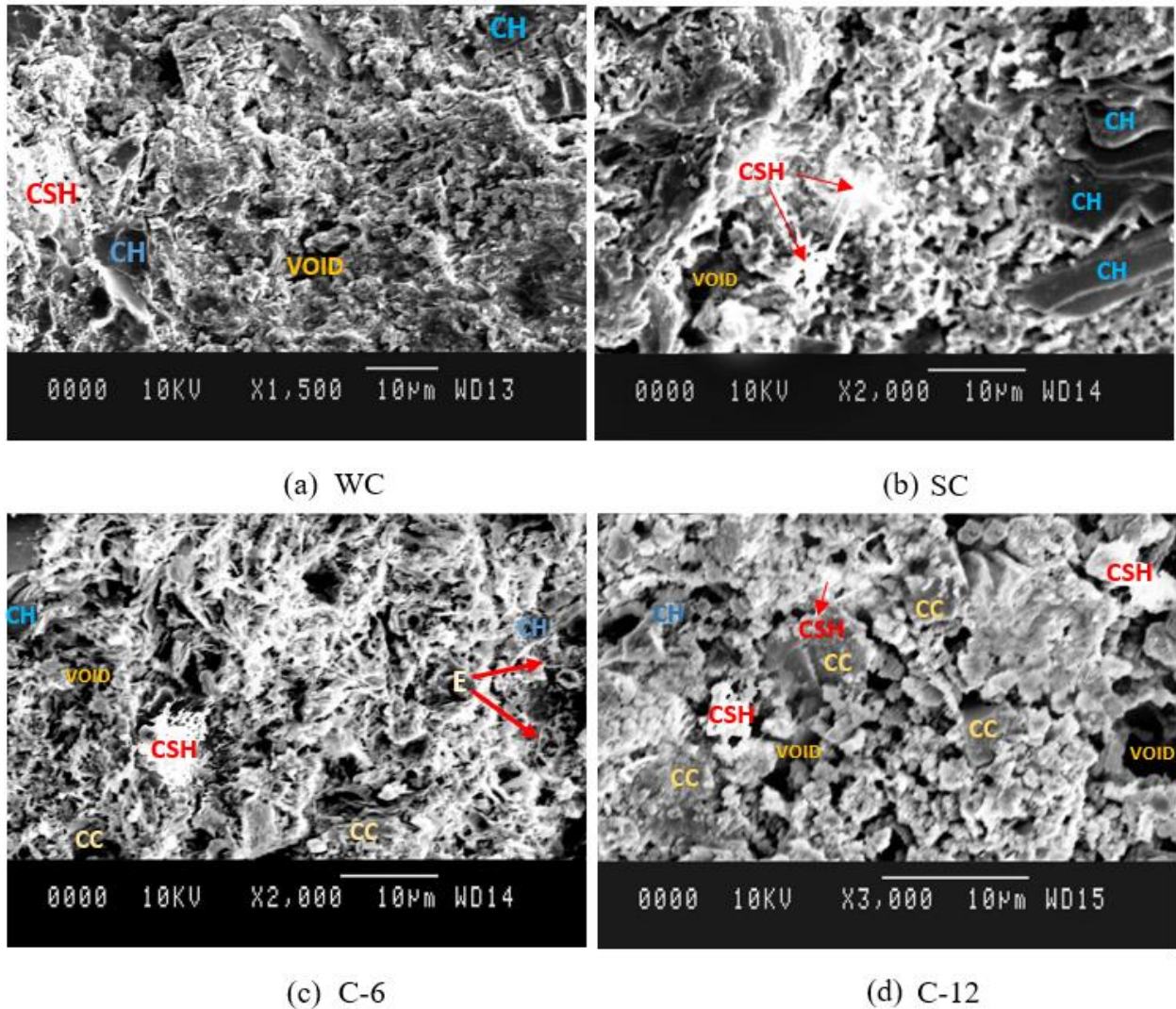


Figure 4.10: SEM analysis of four different curing regimes at the age of 28-days of casting

C-12 specimen image Figure 4.10(d) shows the presence of CaCO_3 formed due to ACC and additional CSH gel formed due to sufficient moisture provided by 3-day water curing for hydration reaction to carry out at later ages. Presence of CaCO_3 densifies the microstructure due to its higher density and volume as compared to conventional hydration products. Additional CSH provided by subsequent WC following ACC further densifies the microstructure. C-6 specimen shows the presence of a reduced amount of CaCO_3 and CSH as compared to C-12. SC specimen shows the relatively denser structure as compared to WC counterparts due to higher CSH formed during initial steam curing and subsequent water curing till testing age.

4.8 APPLICATION OF DEVELOPED PERVIOUS CONCRETE IN PAVER BLOCKS

Pervious concrete has been used in a variety of applications, notable among which are low-traffic pavements such as parking lots and sidewalks, around buildings, and on highway shoulders and medians. Other applications include greenhouse floors to keep the floor free of standing water, surface course for tennis courts, zoo areas, swimming pool decks, beach structures, seawalls, and embankments (*Sonebi et al., 2016*).

Application of developed pervious concrete in paver blocks, shown in Figure 4.11 was studied. Compressive strength and porosity tests results of paver blocks are presented in subsequent sections.

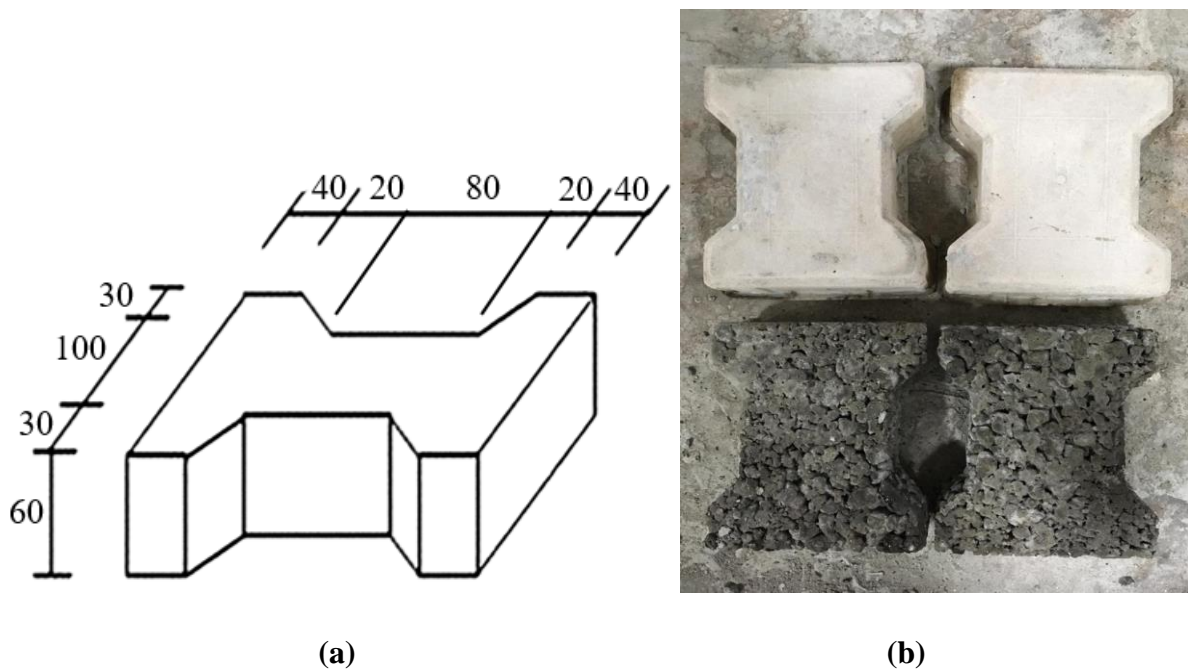


Figure 4.11: Interlocking tile specimen (a) Dimensions (b) After demoulding

4.8.1 Compressive strength of paver blocks

Compressive strength test of pervious concrete specimens cured under different curing regimes was conducted at the ages of 3, 7 and 28-days of casting and the results are presented in Table 4.5 and Figure 4.12. The compressive strength of paver blocks attained by all the curing regimes was higher than the minimum required compressive strength of 10 MPa for drainage pavement, precast concrete products and stone protection (*Rafique et al., 2012*). Compressive strength test results of paver blocks have a similar trend as observed in compressive strength test results of cubes at all the curing ages.

Table 4.5: Compressive strength test results at the ages of 3,7 and 28-days of casting

Curing scheme	Compressive strength (MPa)			% increase in compressive strength w.r.t water curing regime		
	3-days	7-days	28-days	3-days	7-days	28-days
WC	11.19	14.85	16.98	-	-	-
SC	16.69	18.04	20.19	+49.15	+21.48	+18.90
C-6	12.37	14.13	16.10	+10.54	-4.84	-5.18
C-12	16.08	20.27	23.76	+43.70	+36.50	+39.93

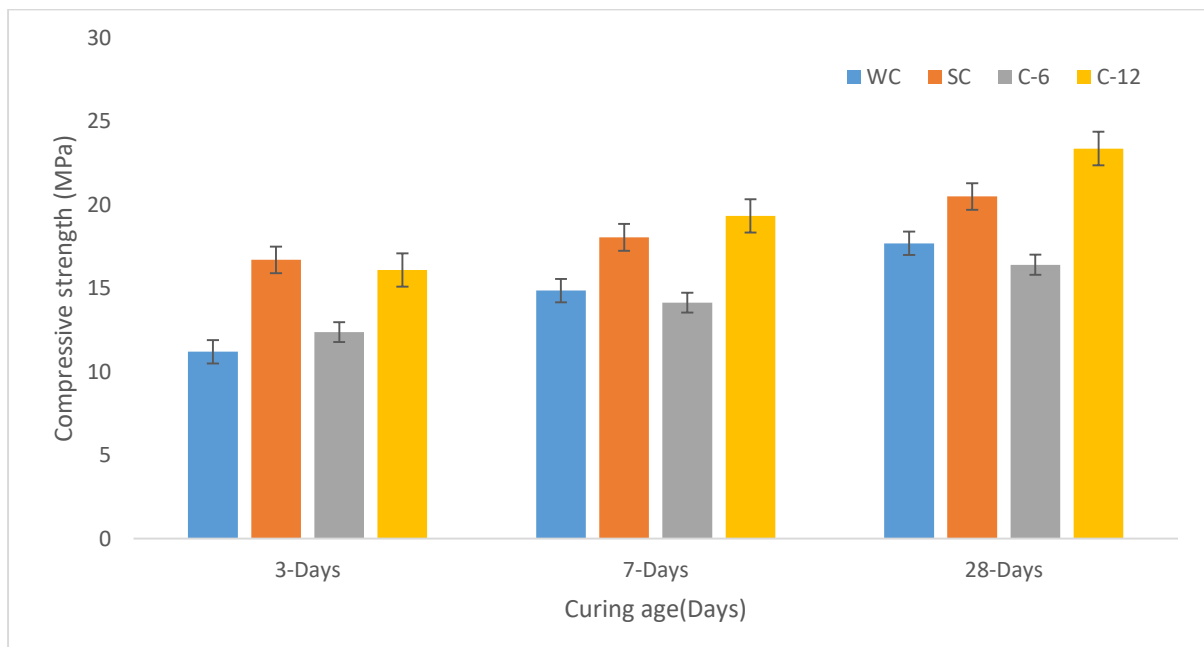


Figure 4.12: Compressive strength test results at the ages of 3, 7 and 28-days of casting

4.8.2 Porosity of paver blocks

Porosity test of pervious concrete specimens cured under different curing regimes was conducted at the ages of 3, 7 and 28-days of casting and the results are presented in Table 4.6 and Figure 4.13. The porosity of paver blocks varied from 12.24 to 24.97 % irrespective of curing regimes, which is acceptable as recommended porosity ranges from 15 to 25 % (*Rafique et al., 2012*). Porosity test results of paver blocks have a similar trend as observed in porosity test results of cubes at all the curing ages.

Table 4.6: Porosity test results at the ages of 3, 7 and 28-days of casting

Curing scheme	Porosity (%)			% increase in porosity w.r.t water curing regime		
	3-day	7-day	28-day	3-day	7-day	28-day
WC	21.86	19.32	18.8	-	-	-
SC	24.97	20.34	18.28	+14.23	+5.28	-2.765
C-6	18.83	17.49	16.79	-13.86	-9.47	-10.69
C-12	15.79	13.55	12.24	-27.90	-29.86	-34.89

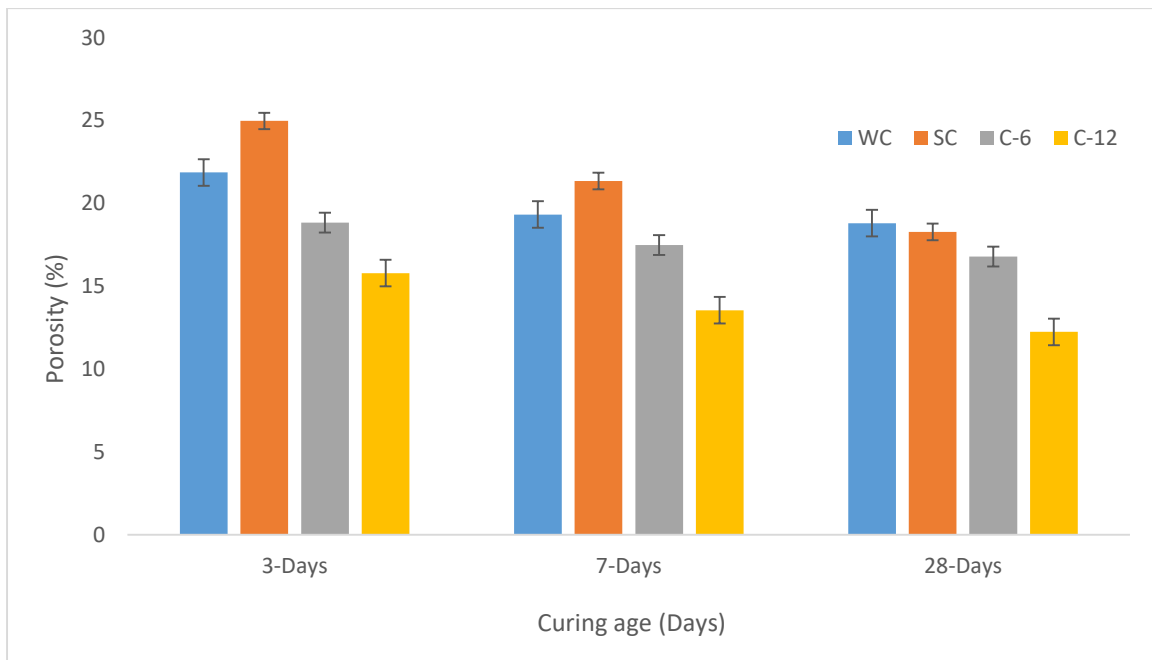


Figure 4.13: Porosity test results at the ages of 3, 7 and 28-days of casting

CHAPTER 5 - CONCLUSION

5.1 GENERAL

In this study, the effect of accelerated carbonation curing on the compressive strength, porosity, and permeability of pervious concrete was investigated and was compared with steam curing and water curing. Microstructure analysis of the pervious concrete specimens was done using TGA, XRD and SEM techniques. The developed pervious concrete was applied in pervious concrete paver blocks, and compressive strength and porosity of pervious concrete paver blocks were also studied. On the basis of the results obtained from the present study, the following conclusions were drawn.

5.2 COMPRESSIVE STRENGTH

The compressive strength at 3-days of casting was highest for steam cured specimen, followed by ACC cured. Steam cured had 49.5% higher compressive strength than water cured counterpart. This was attributed to a higher rate of hydration at the elevated temperature for the steam cured specimen.

The accelerated carbonation cured specimen (C-12) showed the highest compressive strength at 7 and 28-days, followed by the steam cured specimen. This was credited to the formation of CaCO_3 during ACC and additional CSH on subsequent water curing. While 3-days strength of steam cured was considerably higher than water cured, the difference reduced with curing age and was not significant at the age of 28-days of casting.

The accelerated carbonation cured specimen (C-6) had the lowest compressive strength at 7 and 28-days. This was due to the lesser duration of ACC, which resulted in sufficient carbonation at near-surface of cement paste; however, enough carbonation hasn't occurred in depth of cement paste.

5.3 POROSITY

The porosity test showed the lowest values for accelerated carbonation cured specimens at all curing ages. This was attributed to the formation of CaCO_3 during ACC, which has a higher volume and density as compared to conventional hydration products.

Steam and water cured specimens had the highest porosity at all curing ages. The difference in porosity between two curing regimes reduced with age. Steam cured had higher porosity at the age of 3 and 7-days of casting, while at 28-day water cured had slightly higher porosity than steam cured specimen.

5.4 PERMEABILITY

Permeability test was conducted at the ages of 3, 7 and 28 days. The results of permeability were quite similar to the results obtained in porosity tests. The permeability test showed the lowest values for accelerated carbonation cured specimens at all curing ages. This was attributed to the formation of CaCO_3 during ACC, which creates a micro-aggregate effect and causes clogging of pores.

Steam and water cured specimens showed the highest permeability at all curing ages. The difference in permeability between two curing regimes reduced with age. Steam cured has higher permeability at the age of 3 and 7-days of casting, while at 28-day water cured has slight higher permeability than steam cured specimen. This was due to the fact that elevated temperature causes micro-cracks and also results in non-uniform distribution of hydration products in case of the steam cured specimen. Subsequent water curing of Steam cured specimens till the age of testing leads to more uniform of distribution of hydration products and thus, reducing porosity and permeability.

5.5 MICROSTRUCTURE ANALYSIS

5.5.1 TGA analysis

TGA analysis exhibited more CO_2 uptake, and higher calcium carbonate and calcium hydroxide formation in C-12 specimen as compared to C-6 specimen. This was attributed to the higher duration of ACC in C-12, which leads to more CO_2 sequestration into C-12 specimen.

5.5.2 XRD analysis

The major phases identified in the XRD analysis were Quartz (SiO_2), calcium hydroxide (Ca(OH)_2), calcium carbonate (CaCO_3), tri-calcium silicate (C_3S) and di-calcium silicate (C_2S).

XRD analysis of WC regime showed strong peaks of calcium hydroxide (Ca(OH)_2), quartz, tri-calcium silicate (C_3S) and di-calcium silicate (C_2S). The intensity of CH Peaks was lesser for WC as compared to SC due to the higher rate of hydration in SC, and subsequent water curing in SC regime aids hydration of cement. XRD analysis shows strong peaks of quartz and CH in SC specimen as compared to other curing regimes.

Calcium carbonate peaks were observed in accelerated carbonation cured specimens. C-12 specimen showed diminished peaks of Ca(OH)_2 due to the conversion of Ca(OH)_2 to CaCO_3 by CO_2 during carbonation at the age of 3-days, and at 28 days peaks of Ca(OH)_2 in C-12 confirms, further hydration on subsequent water curing following ACC. Strong peaks of CaCO_3 confirms sufficient carbonation of C-12 specimen. The intensity of CaCO_3 peaks was lesser in C-6 specimen as compared to C-12. This further confirms that 6 hours duration of ACC was not enough for sufficient carbonation of cement paste.

5.5.3 SEM analysis

SEM analysis showed accelerated carbonation cured specimen (C-12) had denser microstructure as compared to other curing regimes. ACC causes a reaction between carbon dioxide and calcium hydroxide, with calcium carbonate as the end product. Calcium carbonate leads to denser microstructure due to its higher density than calcium hydroxide. Subsequent water curing of C-12 specimen further aids hydration and provide additional CSH which further densify the microstructure.

Steam cured specimen SEM images showed more presence of CSH and denser microstructure as compared to WC specimen at the age of 28-days of casting. This was in agreement with compressive strength and porosity results.

5.6 APPLICATION OF PERVIOUS CONCRETE TO PAVER BLOCKS

The developed pervious concrete from the tests was applied to paver interlocking paver blocks. Pervious concrete cubes and paver blocks had shown higher compressive strength than required 10 MPa for all curing regimes (*Rafique et al., 2012*). Therefore, paver blocks made from pervious concrete could be used for application as paver blocks to sidewalks and drainage pavements.

REFERENCES

- Ahmad, S., 2018. sequestration, Epigenetic Biomarkers and Diagnostics. Elsevier Ltd.
<https://doi.org/10.1016/B978-0-08-102444-7.00005-8>
- Ahmad, S., Assaggaf, R.A., Maslehuddin, M., Al-amoudi, O.S.B., Adekunle, S.K., Ali, S.I., 2017. Effects of carbonation pressure and duration on strength evolution of concrete subjected to accelerated carbonation curing. *Constr. Build. Mater.* 136, 565–573.
<https://doi.org/10.1016/j.conbuildmat.2017.01.069>
- Alexanderson, J., 1972. Strength losses in heat cured concrete. *Swedish Cem. Concr. Res. Inst.*
- Ba, M., Qian, C., Guo, X., Han, X., 2011. Effects of steam curing on strength and porous structure of concrete with low water / binder ratio. *Constr. Build. Mater.* 25, 123–128.
<https://doi.org/10.1016/j.conbuildmat.2010.06.049>
- Babu, T.S.R., Neeraja, D., 2017. Case Studies in Construction Materials A experimental study of natural admixture effect on conventional concrete and high volume class F fl yash blended concrete. *Case Stud. Constr. Mater.* 6, 43–62.
<https://doi.org/10.1016/j.cscm.2016.09.003>
- Baojian, Z., Chisun, P., Caijun, S., 2013. Cement & Concrete Composites CO 2 curing for improving the properties of concrete blocks containing recycled aggregates 42, 1–8.
<https://doi.org/10.1016/j.cemconcomp.2013.04.013>
- Barišić, I., Galić, M., Grubeša, I.N., 2017. Pervious concrete mix optimization for sustainable pavement solution.
- BUREAU OF INDIAN STANDARDS, 2004. IS 516 -1959: Method of Tests for Strength of Concrete. IS 516 -1959 Method Tests Strength Concr.
- Chabannes, M., Garcia-diaz, E., Clerc, L., Bénézet, J., 2015. Studying the hardening and mechanical performances of rice husk and hemp-based building materials cured under natural and accelerated carbonation 94, 105–115.
<https://doi.org/10.1016/j.conbuildmat.2015.06.032>
- Deogekar, P., Jain, A., Nanthagopalan, P., 2013. Influence of Steam Curing Cycle on

Compressive strength of Concrete.

- Ducman, V., Korat, L., Netinger, I., Barišić, I., 2018. Draining capability of single-sized pervious concrete 169, 252–260. <https://doi.org/10.1016/j.conbuildmat.2018.03.037>
- Guo, M., Tu, Z., Sun, C., Shi, C., 2018. Improvement of properties of architectural mortars prepared with 100 % recycled glass by CO₂ curing 179, 138–150.
- Hanh, D., Boutouil, M., Sebaibi, N., Baraud, F., Leleyter, L., 2020. Durability of pervious concrete using crushed seashells 135, 137–150.
- Hanson, J., 1963. Optimum Steam Curing Procedure in Precasting Plants. *ACI J. Proc.* 60. <https://doi.org/10.14359/7843>
- He, P., Shi, C., Tu, Z., Sun, C., Zhang, J., 2016. Effect of further water curing on compressive strength and microstructure of CO₂-cured concrete Effect of further water curing on compressive strength and microstructure of CO₂ -cured concrete. *Cem. Concr. Compos.* 72, 80–88. <https://doi.org/10.1016/j.cemconcomp.2016.05.026>
- He, Z., Li, Z., Shao, Y., 2017. Effect of carbonation mixing on CO₂ uptake and strength gain in concrete. *J. Mater. Civ. Eng.* 29. [https://doi.org/10.1061/\(ASCE\)MT.1943-5533.0002031](https://doi.org/10.1061/(ASCE)MT.1943-5533.0002031)
- Hernández-Bautista, E., Sandoval-Torres, S., Cano-Barrita, P.F. d. J., Bentz, D.P., 2017. Modeling heat and moisture transport in steam-cured mortar: Application to AASHTO Type VI beams. *Constr. Build. Mater.* 151, 186–195. <https://doi.org/10.1016/j.conbuildmat.2017.05.151>
- Huntzinger, D.N., Gierke, J.S., Sutter, L.L., Kawatra, S.K., Eisele, T.C., 2009. Mineral carbonation for carbon sequestration in cement kiln dust from waste piles 168, 31–37. <https://doi.org/10.1016/j.jhazmat.2009.01.122>
- Mironov, S.A., 1966. Some generalizations in theory and technology of acceleration of concrete hardening. *Highw. Res. Board Spec. Rep.* 465–474.
- Mo, L., Zhang, F., Deng, M., Jin, F., Al-tabbaa, A., Wang, A., 2017. Accelerated carbonation and performance of concrete made with steel slag as binding materials and aggregates. *Cem. Concr. Compos.* 83, 138–145. <https://doi.org/10.1016/j.cemconcomp.2017.07.018>

- Neves, A., Dias, R., Filho, T., Moraes, E. De, Fairbairn, R., Dweck, J., 2015. The effects of the early carbonation curing on the mechanical and porosity properties of high initial strength Portland cement pastes 77, 448–454.
- Panesar, D.K., Mo, L., 2013. Properties of binary and ternary reactive MgO mortar blends subjected to CO₂ curing. *Cem. Concr. Compos.* 38, 40–49.
<https://doi.org/10.1016/j.cemconcomp.2013.03.009>
- Qian, L., Jiayang, L., Liqian, Q., 2016. Effects of temperature and carbonation curing on the mechanical properties of steel slag-cement binding materials. *Constr. Build. Mater.* 124, 999–1006. <https://doi.org/10.1016/j.conbuildmat.2016.08.131>
- Rafique, M.A., Tsuruta, K., Mirza, J., 2012. Evaluation of high-performance porous concrete properties. *Constr. Build. Mater.* 31, 67–73.
<https://doi.org/10.1016/j.conbuildmat.2011.12.024>
- Ramkrishnan, R., Abilash, B., Trivedi, M., Varsha, P., Varun, P., Vishanth, S., 2018. ScienceDirect Effect of Mineral Admixtures on Pervious Concrete. *Mater. Today Proc.* 5, 24014–24023. <https://doi.org/10.1016/j.matpr.2018.10.194>
- Rangelov, M., Nassiri, S., Chen, Z., Russell, M., Uhlmeier, J., 2017. Quality Evaluation Tests for Pervious Concrete Pavements ' Placement. *Int. J. Pavement Res. Technol.*
<https://doi.org/10.1016/j.ijprt.2017.01.007>
- Rostami, V., Shao, Y., Boyd, A.J., 2012. Carbonation Curing versus Steam Curing for Precast Concrete Production 24, 1221–1229. [https://doi.org/10.1061/\(ASCE\)MT.1943-5533.0000462](https://doi.org/10.1061/(ASCE)MT.1943-5533.0000462).
- Rostami, V., Shao, Y., Boyd, A.J., 2011. Durability of concrete pipes subjected to combined steam and carbonation curing 25, 3345–3355.
<https://doi.org/10.1016/j.conbuildmat.2011.03.025>
- Sandoval, G.F.B., Galobardes, I., Teixeira, R.S., Toralles, B.M., 2017. Case Studies in Construction Materials Comparison between the falling head and the constant head permeability tests to assess the permeability coefficient of sustainable Pervious Concretes 7, 317–328.

- Sharma, D., Goyal, S., 2018. Accelerated carbonation curing of cement mortars containing cement kiln dust : An effective way of CO₂ sequestration and carbon footprint reduction. *J. Clean. Prod.* 192, 844–854. <https://doi.org/10.1016/j.jclepro.2018.05.027>
- Shen, P., Lu, L., Chen, W., Wang, F., Hu, S., 2017. Efficiency of metakaolin in steam cured high strength concrete. *Constr. Build. Mater.* 152, 357–366. <https://doi.org/10.1016/j.conbuildmat.2017.07.006>
- Sonebi, M., Bassuoni, M., Yahia, A., 2016. *Pervious Concrete : Mix Design , Properties and Applications* 109–115.
- www.ccanz.org.nz [WWW Document], n.d. URL <https://www.ccanz.org.nz/page/Curing-Methods.aspx>
- www.nbmw.com, n.d.
- Xu, G., Shen, W., Huo, X., Yang, Z., Wang, J., Zhang, W., Ji, X., 2018. Investigation on the properties of porous concrete as road base material. *Constr. Build. Mater.* 158, 141–148. <https://doi.org/10.1016/j.conbuildmat.2017.09.151>
- Yan, X., Jiang, L., Guo, M., Chen, Y., Song, Z., Bian, R., 2019. Evaluation of sulfate resistance of slag contained concrete under steam curing. *Constr. Build. Mater.* 195, 231–237. <https://doi.org/10.1016/j.conbuildmat.2018.11.073>
- Yap, S.P., Zhao, P., Chen, C., Goh, Y., Ibrahim, H.A., Mo, K.H., Yuen, C.W., 2018. Characterization of pervious concrete with blended natural aggregate and recycled concrete aggregates. <https://doi.org/10.1016/j.jclepro.2018.01.205>
- Yeih, W., Jhy, J., 2019. The influences of cement type and curing condition on properties of pervious concrete made with electric arc furnace slag as aggregates. *Constr. Build. Mater.* 197, 813–820. <https://doi.org/10.1016/j.conbuildmat.2018.08.178>
- Zhang, D., Ghoulah, Z., Shao, Y., 2017. Review on carbonation curing of cement-based materials. *J. CO₂ Util.* 21, 119–131. <https://doi.org/10.1016/j.jcou.2017.07.003>
- Zhang, D., Shao, Y., 2016. Effect of early carbonation curing on chloride penetration and weathering carbonation in concrete. *Constr. Build. Mater.* 123, 516–526. <https://doi.org/10.1016/j.conbuildmat.2016.07.041>

Zhi-min, H.E., Guang-cheng, L., You-jun, X.I.E., 2012. Influence of subsequent curing on water sorptivity and pore structure of steam-cured concrete 1155–1162.

<https://doi.org/10.1007/s11771-012-1122-2>

Zhong, R., Leng, Z., Poon, C., 2018. Research and application of pervious concrete as a sustainable pavement material : A state-of-the-art and state-of-the-practice review.

Constr. Build. Mater. 183, 544–553. <https://doi.org/10.1016/j.conbuildmat.2018.06.131>

Zou, C., Long, G., Ma, C., Xie, Y., 2018. Effect of subsequent curing on surface permeability and compressive strength of steam-cured concrete. Constr. Build. Mater. 188, 424–432.

<https://doi.org/10.1016/j.conbuildmat.2018.08.076>